

Label Distribution Learning using the Squared Neural Family on the Probability Simplex

Daokun Zhang¹, Russell Tsuchida², and Dino Sejdinovic³

¹School of Computer Science, University of Nottingham Ningbo China

²Data61, CSIRO, Australia

³School of Computer and Mathematical Sciences, The University of
Adelaide

Abstract

Label distribution learning (LDL) provides a framework wherein a distribution over categories rather than a single category is predicted, with the aim of addressing ambiguity in labeled data. Existing research on LDL mainly focuses on the task of point estimation, i.e., pinpointing an optimal distribution in the probability simplex conditioned on the input sample. In this paper, we estimate a probability distribution of all possible label distributions over the simplex, by unleashing the expressive power of the recently introduced Squared Neural Family (SNEFY). With the modeled distribution, label distribution prediction can be achieved by performing the expectation operation to estimate the mean of the distribution of label distributions. Moreover, more information about the label distribution can be inferred, such as the prediction reliability and uncertainties. We conduct extensive experiments on the label distribution prediction task, showing that our distribution modeling based method can achieve very competitive label distribution prediction performance compared with the state-of-the-art baselines. Additional experiments on active learning and ensemble learning demonstrate that our probabilistic approach can effectively boost the performance in these settings, by accurately estimating the prediction reliability and uncertainties.

1 Introduction

Label distribution learning (LDL) is a technique which handles ambiguity in multi-class classification, by utilising simplex-valued rather than categorical-valued labels in training

data. Unlike traditional multi-class and multi-label learning paradigms, which assign a deterministic label prediction to instances, LDL corresponds to the question “*How well does each of the labels describe an instance?*”, by using a discrete probability distribution to characterize the instance’s affinity to all candidate categories. For example, when we predict the functionality of a district in a city, we might predict a result such as: the district has 20% functionality for business, 40% functionality for entertainment, and 40% functionality for education.

Many LDL algorithms have been proposed to directly predict label distribution vectors from instance features, by adapting machine learning algorithms designed for “hard” label prediction to the “soft” label prediction setting. Though a discrete distribution among candidate labels is predicted, existing LDL algorithms still operate at the level of point estimation, i.e., they search for a single point on a probability simplex (the set of all possible label distributions) for each given instance. The point estimation paradigm is particularly susceptible to data uncertainty and inexact mappings between instances and labels, due to the inherent complexity of the data collection and generation processes. Therefore, modeling the probability distribution of label distribution vectors, i.e., the probability distribution supported on the probability simplex, is an important step towards trustworthy LDL. An additional bonus of the distribution modeling is the ability to quantify the prediction reliability and uncertainties, which not only facilitates reliable model deployment in real-world safety critical applications, but is also essential to various reliability/uncertainty-aware tasks, like pseudo labeling, active learning, and ensemble learning.

Contributions In this paper, we propose a novel LDL framework, SNEFY-LDL, by unleashing the probability modeling power of the recently proposed Squared Neural Family (SNEFY) [Tsuchida et al., 2023], a new class of tractable probability models. By restricting the support set of SNEFY to a probability simplex, SNEFY-LDL provides an expressive conditional distribution modeling of the label distribution vector given the input sample. The conditional distribution model has a closed-form normalizing constant, guaranteeing computational tractability. In this way, model parameters can be learned efficiently by maximizing the conditional likelihoods of training samples with stochastic gradient descent. Through computing the expectation of the conditional distribution, we can obtain the closed-form distribution mean, as a way to summarize the fitted model and predict label distributions for unlabeled samples. However, this is only one way to use the fitted model and the probability density values can be used to evaluate the reliability of label distribution predictions.

We conduct extensive experiments on fourteen real-world datasets to evaluate the label distribution prediction performance of the proposed SNEFY-LDL model. Experimental

results show that SNEFY-LDL can achieve very competitive label distribution prediction performance, compared with the state-of-the-art LDL baselines. In addition, label distribution active learning and ensemble learning experiments are carried out to verify the efficacy of SNEFY-LDL in quantifying prediction uncertainties. The max-entropy principle is used to achieve active learning with the estimated SNEFY-LDL entropy, i.e., select the most informative unlabeled samples with the largest entropy values, query their labels and augment training samples, to attain the largest performance gain of the re-trained LDL model. Experimental results show that the max-entropy principle achieves significantly better active learning performance than the representativeness based active learning baselines. The experiments on ensemble learning demonstrate that SNEFY-LDL gives a further usecase for the fitted probabilistic model, as it provides an intelligent mechanism for weighting base learners, significantly outperforming the uniform weighting strategy.

2 Related Work

LDL is first proposed by [Geng et al., 2013] to solve the facial age estimation problem with insufficient training samples. Since then, a series of LDL algorithms have been developed, which can be divided into three categories: Problem Transformation (PT), Algorithm Adaptation (AA) and Specialized Algorithms (SA) [Geng, 2016].

Problem Transformation PT [Geng, 2016] transforms the LDL problem into the single-label classification problem, by decomposing each training sample assigned with a label distribution into a set of duplicate training samples. Each of them is assigned with a different label and accounts for a partial sample in proportion to the label probability value, and is then used to train the single-label classifiers. The label likelihoods predicted by the single-label classifiers are then aggregated to form the final prediction of label distributions. PT-Bayes [Geng, 2016] and PT-SVM [Geng, 2016, Geng and Hou, 2015] transform the LDL problem into the single-label multi-class classification problem and respectively employ Bayes and SVM as the single-label classifiers. DF-LDL [González et al., 2021a] decomposes the label distribution prediction task into a number of one-versus-one binary classification tasks, and fuses the binary classification likelihoods to form the final label distribution prediction.

Algorithm Adaptation AA [Geng, 2016] adapts traditional single-label classification models into the LDL setting, by leveraging the models’ compatibility in outputting a soft label distribution vector. Derived from the K Nearest Neighbor (KNN) algorithm [Wu et al., 2008], AA-KNN [Geng, 2016] predicts samples’ label distributions by averaging the label

distributions of their k nearest neighbors in feature space. AA-BP [Geng, 2016] constructs a three-layer neural network and adopts the softmax function as the activation of the output layer, making the neural network naturally produce a label distribution for each example. The neural network is trained by minimizing the sum of squared errors between the model output label distributions and the ground-truth label distributions.

Specialized Algorithms SA [Geng, 2016] designs algorithms from scratch to directly solve the LDL problem. SA-IIS [Geng et al., 2013] and SA-BFGS [Geng, 2016] use the maximum entropy model to parameterize label distributions. They are trained by minimizing the Kullback-Leibler (KL) divergence between the model output and ground-truth label distributions, where Improved Iterative Scaling (IIS) [Malouf, 2002] and BFGS [Nocedal and Wright, 1999] are respectively leveraged by SA-IIS and SA-BFGS as optimizers. CPNN [Geng et al., 2013] uses a neural network to parameterize the joint probability distribution between sample features and labels following Modha’s probability distribution formulation [Modha and Fainman, 1994]. BCPNN [Yang et al., 2017] and ACPNN [Yang et al., 2017] then improve on CPNN through leveraging binary label encoding and augmenting training samples respectively. LDLF [Shen et al., 2017] employs differentiable decision trees [Kontschieder et al., 2015] to model label distributions and KL divergence is used to design the learning objective. LDL-SCL [Jia et al., 2021] forces the label distributions of samples located closely in feature space to be similar to each other. LDL-LRR [Jia et al., 2023b] and LDL-DPA [Jia et al., 2023a] maintain the relative importance ranking between different labels in label distribution modeling, by penalizing a label importance ranking loss in their learning objectives.

Extensions In addition, LDL has been extended to other tasks, like label enhancement (recovering label distributions from the one-hot single-label assignments) [Xu et al., 2019b, 2020, Zheng et al., 2023], multi-class classification [Wang and Geng, 2019, 2021b,a], learning with incomplete supervision [Xu and Zhou, 2017], oversampling [González et al., 2021b], ordinal LDL [Wen et al., 2023], semi-supervised learning [Xie et al., 2023], and label calibration [He et al., 2024]. Furthermore, LDL has been applied to solve numerous real-world problems, including facial age estimation [Geng et al., 2013], facial emotion recognition [Chen et al., 2020], head pose estimation [Xu et al., 2019a], crowd opinion prediction [Geng and Hou, 2015], emphasis selection [Shirani et al., 2019], lesion counting [Wu et al., 2019], and urban function distribution [Huang et al., 2023]. It is worth noting that there is a related topic in the classical statistics literature, termed *compositional data analysis* [Greenacre, 2021], with a broad range of applications including geochemistry (e.g. labels correspond to mineral compositions) and ecology (e.g. labels correspond to relative abundance of species).

However, existing LDL algorithms mainly fall into the regime of point estimation. They discover an optimal discrete label distribution in the probability simplex with regard to a predefined learning objective, and do not provide the information about how prominent the optimal label distribution is, compared with the remaining distribution candidates. In this paper, we aim to model the distribution of label distributions, with the expectation that we can provide a promising mechanism for LDL uncertainty quantification.

3 Problem Definition

Assume we are given a set of N i.i.d training samples $\mathcal{X} = \{\mathbf{x}_1, \mathbf{x}_2, \dots, \mathbf{x}_N\}$ with each sample $\mathbf{x} \in \mathcal{X}$ located in the d -dimensional Euclidean space \mathbb{R}^d . In addition, each sample $\mathbf{x} \in \mathcal{X}$ is described by a L -dimensional label distribution vector $\boldsymbol{\ell}_x \in \mathbb{R}^L$ that takes values in the $(L - 1)$ -simplex Δ^{L-1} , corresponding to a set of L given labels $\mathcal{Y} = \{y_1, y_2, \dots, y_L\}$. The l -th entry $\ell_x^{y_l}$ of the label distribution vector $\boldsymbol{\ell}_x$ corresponds to the probability of sample \mathbf{x} belonging to the l -th class y_l , i.e., $\ell_x^{y_l} = P(y_l|\mathbf{x}) \geq 0$, satisfying the constraint that $\sum_{l=1}^L \ell_x^{y_l} = 1$.

With the label distribution observations of training samples, our objective is to model the probability distribution of the label distribution vector $\boldsymbol{\ell} \in \Delta^{L-1}$ conditioned on any input sample $\mathbf{x} \in \mathbb{R}^d$, $P(d\boldsymbol{\ell}|\mathbf{x})$.

For any sample $\mathbf{x} \in \mathbb{R}^d$ with an unknown label distribution, one can associate to it a label distribution vector $\boldsymbol{\ell}_x^*$ obtained as the mean of the fitted distribution $P(d\boldsymbol{\ell}|\mathbf{x})$:

$$\boldsymbol{\ell}_x^* = \int_{\Delta^{L-1}} \boldsymbol{\ell} P(d\boldsymbol{\ell}|\mathbf{x}), \quad (1)$$

but the fitted model $P(d\boldsymbol{\ell}|\mathbf{x})$ can serve many other purposes.

4 Preliminaries on SNEFY

Given a measure space $(\Omega, \mathcal{F}, \mu)$ with set Ω , sigma algebra \mathcal{F} , and nonnegative measure μ , SNEFY defines a probability distribution P on some support $\mathcal{Z} \in \mathcal{F}$ to be proportional to the evaluation of the squared 2-norm of a neural network \mathbf{f} :

$$P(d\mathbf{z}; \mathbf{V}, \boldsymbol{\Theta}) \triangleq \frac{\|\mathbf{f}(\mathbf{t}(\mathbf{z}); \mathbf{V}, \boldsymbol{\Theta})\|_2^2 \mu(d\mathbf{z})}{\int_{\mathcal{Z}} \|\mathbf{f}(\mathbf{t}(\mathbf{z}); \mathbf{V}, \boldsymbol{\Theta})\|_2^2 \mu(d\mathbf{z})}, \quad (2)$$

$$\mathbf{f}(\mathbf{t}(\mathbf{z}); \mathbf{V}, \boldsymbol{\Theta}) = \mathbf{V} \sigma(\mathbf{W}\mathbf{t}(\mathbf{z}) + \mathbf{b}), \quad \boldsymbol{\Theta} = (\mathbf{W}, \mathbf{b}),$$

where $\mathbf{t}(\cdot) : \mathcal{Z} \rightarrow \mathbb{R}^D$ is the sufficient statistic, σ is the activation function, $\mathbf{W} \in \mathbb{R}^{n \times D}$ and $\mathbf{b} \in \mathbb{R}^n$ are respectively the weight matrix and bias vector at the hidden layer of neural network \mathbf{f} , and $\mathbf{V} \in \mathbb{R}^{m \times n}$ are \mathbf{f} 's readout parameters. $\Theta = (\mathbf{W}, \mathbf{b}) \in \mathbb{R}^{n \times (D+1)}$ denotes the concatenation of \mathbf{W} and \mathbf{b} and its i th row is denoted as $\theta_i = (\mathbf{w}_i, b_i) \in \mathbb{R}^{D+1}$.

The distribution $P(d\mathbf{z}; \mathbf{V}, \Theta)$ in Eq. (2) admits a more concise formulation

$$\begin{aligned} P(d\mathbf{z}; \mathbf{V}, \Theta) &= \frac{\text{Tr}[\mathbf{V}^\top \mathbf{V} \widetilde{\mathbf{K}}_\Theta(\mathbf{z})]}{\text{Tr}[\mathbf{V}^\top \mathbf{V} \mathbf{K}_\Theta]} \mu(d\mathbf{z}), \\ &= \frac{\text{vec}(\mathbf{V}^\top \mathbf{V})^\top \text{vec}(\widetilde{\mathbf{K}}_\Theta(\mathbf{z}))}{\text{vec}(\mathbf{V}^\top \mathbf{V})^\top \text{vec}(\mathbf{K}_\Theta)} \mu(d\mathbf{z}), \end{aligned} \quad (3)$$

where $\widetilde{\mathbf{K}}_\Theta(\mathbf{z}) \in \mathbb{R}^{n \times n}$ is a positive semidefinite (PSD) matrix, whose ij th element is a kernel function of θ_i and θ_j :

$$\tilde{k}_{\sigma, \mathbf{t}}(\theta_i, \theta_j; \mathbf{z}) = \sigma(\mathbf{w}_i^\top \mathbf{t}(\mathbf{z}) + b_i) \sigma(\mathbf{w}_j^\top \mathbf{t}(\mathbf{z}) + b_j), \quad (4)$$

while \mathbf{K}_Θ is the elementwise integral of $\widetilde{\mathbf{K}}_\Theta(\mathbf{z})$, preserving the PSD property, with its ij th entry formulated as another kernel function of θ_i and θ_j :

$$\mathbf{k}_{\sigma, \mathbf{t}, \mu}(\theta_i, \theta_j) = \int_{\mathcal{Z}} \tilde{k}_{\sigma, \mathbf{t}}(\theta_i, \theta_j; \mathbf{z}) \mu(d\mathbf{z}). \quad (5)$$

Under varying choices of the activation function σ , sufficient statistic \mathbf{t} , and the base measure μ , $\mathbf{k}_{\sigma, \mathbf{t}, \mu}(\theta_i, \theta_j)$ is able to be computed in closed form (see Table 1 of [Tsuchida et al., 2023]) in $\mathcal{O}(D)$. This makes SNEFY a tractable probability distribution model, with great expressivity and computational efficiency.

SNEFY also enjoys a closed-form formulation for conditional distributions, under mild conditions.

Theorem 1. [Tsuchida et al., 2023] *Let $\mathbf{z} = (\mathbf{z}_1, \mathbf{z}_2)$ jointly follow a SNEFY distribution, with support set $\mathcal{Z} = \mathcal{Z}_1 \times \mathcal{Z}_2$, sufficient statistic \mathbf{t} , activation function σ , base measure μ , as well as parameters \mathbf{V} and $\Theta = ([\mathbf{W}_1, \mathbf{W}_2], \mathbf{b})$. Assume that $\mu(d\mathbf{z}) = \mu_1(d\mathbf{z}_1) \mu_2(d\mathbf{z}_2)$ and $\mathbf{t}(\mathbf{z}) = (\mathbf{t}_1(\mathbf{z}_1), \mathbf{t}_2(\mathbf{z}_2))$. Then the conditional distribution of \mathbf{z}_1 given $\mathbf{z}_2 = \mathbf{z}_2$ is also a SNEFY distribution with support set \mathcal{Z}_1 , sufficient statistic \mathbf{t}_1 , activation function σ , base measure μ_1 , as well as parameters \mathbf{V} and $\Theta_{1|2} = (\mathbf{W}_1, \mathbf{W}_2 \mathbf{t}_2(\mathbf{z}_2) + \mathbf{b})$.*

5 SNEFY-LDL

SNEFY provides an effective way to model the conditional distribution of the label distribution vector $\boldsymbol{\ell} \in \Delta^{L-1}$. We can assume that the concatenation of label distribution vector $\boldsymbol{\ell} \in \Delta^{L-1}$ and its conditioning sample $\boldsymbol{x} \in \mathbb{R}^d$, $\boldsymbol{z} = (\boldsymbol{\ell}, \boldsymbol{x})$, follows a joint SNEFY distribution, with support set $\mathcal{Z} = \Delta^{L-1} \times \mathbb{R}^d$, sufficient statistic $\boldsymbol{t}(\boldsymbol{z}) = (\boldsymbol{t}_1(\boldsymbol{\ell}), \boldsymbol{t}_2(\boldsymbol{x})) : \mathcal{Z} \rightarrow \mathbb{R}^{D_1+D_2}$ composed of $\boldsymbol{t}_1(\cdot) : \Delta^{L-1} \rightarrow \mathbb{R}^{D_1}$ and $\boldsymbol{t}_2(\cdot) : \mathbb{R}^d \rightarrow \mathbb{R}^{D_2}$, activation function σ , base measure $\mu(\boldsymbol{z}) = \mu_1(\boldsymbol{\ell})\mu_2(\boldsymbol{x})$, as well as parameters $\mathbf{V} \in \mathbb{R}^{m \times n}$ and $\Theta = ([\mathbf{W}_1, \mathbf{W}_2], \mathbf{b}) \in \mathbb{R}^{n \times (D_1+D_2+1)}$. Following Theorem 1, given sample \boldsymbol{x} , the conditional distribution of its label distribution vector $\boldsymbol{\ell}$ is a SNEFY distribution with support set Δ^{L-1} , sufficient statistic \boldsymbol{t}_1 , activation function σ , base measure μ_1 , as well as parameters \mathbf{V} and $\Theta_{1|2} = (\mathbf{W}_1, \mathbf{W}_2\boldsymbol{t}_2(\boldsymbol{x}) + \mathbf{b})$. The conditional distribution is

$$\begin{aligned} \mathbb{P}(d\boldsymbol{\ell}|\boldsymbol{x}; \mathbf{V}, \Theta) &\triangleq \frac{\|\mathbf{f}(\boldsymbol{t}_1(\boldsymbol{\ell}), \boldsymbol{t}_2(\boldsymbol{x}); \mathbf{V}, \Theta)\|_2^2 \mu_1(d\boldsymbol{\ell})}{\int_{\Delta^{L-1}} \|\mathbf{f}(\boldsymbol{t}_1(\boldsymbol{\ell}), \boldsymbol{t}_2(\boldsymbol{x}); \mathbf{V}, \Theta)\|_2^2 \mu_1(d\boldsymbol{\ell})}, \\ \mathbf{f}(\boldsymbol{t}_1(\boldsymbol{\ell}), \boldsymbol{t}_2(\boldsymbol{x}); \mathbf{V}, \Theta) &= \mathbf{V}\sigma(\mathbf{W}_1\boldsymbol{t}_1(\boldsymbol{\ell}) + \mathbf{W}_2\boldsymbol{t}_2(\boldsymbol{x}) + \mathbf{b}). \end{aligned} \quad (6)$$

Following Eq. (3), the distribution can be reformulated as

$$\begin{aligned} \mathbb{P}(d\boldsymbol{\ell}|\boldsymbol{x}; \mathbf{V}, \Theta) &= \frac{\text{Tr}[\mathbf{V}^\top \mathbf{V} \widetilde{\mathbf{K}}_\Theta(\boldsymbol{\ell}, \boldsymbol{x})]}{\text{Tr}[\mathbf{V}^\top \mathbf{V} \mathbf{K}_\Theta(\boldsymbol{x})]} \mu_1(d\boldsymbol{\ell}), \\ &= \frac{\text{vec}(\mathbf{V}^\top \mathbf{V})^\top \text{vec}(\widetilde{\mathbf{K}}_\Theta(\boldsymbol{\ell}, \boldsymbol{x}))}{\text{vec}(\mathbf{V}^\top \mathbf{V})^\top \text{vec}(\mathbf{K}_\Theta(\boldsymbol{x}))} \mu_1(d\boldsymbol{\ell}), \end{aligned} \quad (7)$$

where $\widetilde{\mathbf{K}}_\Theta(\boldsymbol{\ell}, \boldsymbol{x}) \in \mathbb{R}^{n \times n}$ is a PSD matrix, with its ij th element being a kernel function of $\boldsymbol{\theta}_i = (\boldsymbol{w}_{1i}, \boldsymbol{w}_{2i}, b_i) \in \mathbb{R}^{D_1+D_2+1}$ and $\boldsymbol{\theta}_j = (\boldsymbol{w}_{1j}, \boldsymbol{w}_{2j}, b_j) \in \mathbb{R}^{D_1+D_2+1}$:

$$\tilde{\mathbf{k}}_{\sigma, \boldsymbol{t}_1, \boldsymbol{t}_2}(\boldsymbol{\theta}_i, \boldsymbol{\theta}_j; \boldsymbol{\ell}, \boldsymbol{x}) = \sigma(\boldsymbol{w}_{1i}^\top \boldsymbol{t}_1(\boldsymbol{\ell}) + \boldsymbol{w}_{2i}^\top \boldsymbol{t}_2(\boldsymbol{x}) + b_i) \cdot \sigma(\boldsymbol{w}_{1j}^\top \boldsymbol{t}_1(\boldsymbol{\ell}) + \boldsymbol{w}_{2j}^\top \boldsymbol{t}_2(\boldsymbol{x}) + b_j), \quad (8)$$

where $\boldsymbol{w}_{1i} \in \mathbb{R}^{D_1}$ and $\boldsymbol{w}_{2i} \in \mathbb{R}^{D_2}$ are respectively the i th row of matrices \mathbf{W}_1 and \mathbf{W}_2 , and b_i is the i th element of the bias vector \mathbf{b} . Then $\mathbf{K}_\Theta(\boldsymbol{x})$ is the elementwise integral of $\widetilde{\mathbf{K}}_\Theta(\boldsymbol{\ell}, \boldsymbol{x})$, preserving the PSD property, with its ij th entry formulated as another kernel function of $\boldsymbol{\theta}_i$ and $\boldsymbol{\theta}_j$:

$$\mathbf{k}_{\sigma, \boldsymbol{t}_1, \boldsymbol{t}_2, \mu_1}(\boldsymbol{\theta}_i, \boldsymbol{\theta}_j; \boldsymbol{x}) = \int_{\Delta^{L-1}} \tilde{\mathbf{k}}_{\sigma, \boldsymbol{t}_1, \boldsymbol{t}_2}(\boldsymbol{\theta}_i, \boldsymbol{\theta}_j; \boldsymbol{\ell}, \boldsymbol{x}) \mu_1(d\boldsymbol{\ell}). \quad (9)$$

By choosing the activation function σ , sufficient statistic \boldsymbol{t}_1 and the base measure μ_1 carefully, the kernel function $\mathbf{k}_{\sigma, \boldsymbol{t}_1, \boldsymbol{t}_2, \mu_1}(\boldsymbol{\theta}_i, \boldsymbol{\theta}_j; \boldsymbol{x})$ admits a closed form, which guarantees that the conditional distribution $\mathbb{P}(d\boldsymbol{\ell}|\boldsymbol{x}; \mathbf{V}, \Theta)$ is tractable. In particular, we have the following

theorem:

Theorem 2. Let $\mathbf{t}_1(\boldsymbol{\ell}) = (\log \ell^{y_1}, \log \ell^{y_2}, \dots, \log \ell^{y_L}) : \Delta^{L-1} \rightarrow \mathbb{R}^L$ by setting $D_1 = L$, the activation function σ be the exponential function \exp , the base measure $\mu_1(d\boldsymbol{\ell}) = d\boldsymbol{\ell}$ be the Lebesgue measure. Under the condition that $\mathbf{W}_1 > -1/2$ elementwise, the kernel function $\mathbf{k}_{\sigma, \mathbf{t}_1, \mathbf{t}_2, \mu_1}(\boldsymbol{\theta}_i, \boldsymbol{\theta}_j; \mathbf{x})$ admits a closed form:

$$\mathbf{k}_{\mathbf{t}_2}(\boldsymbol{\theta}_i, \boldsymbol{\theta}_j; \mathbf{x}) = \exp(\mathbf{w}_{2i}^\top \mathbf{t}_2(\mathbf{x}) + \mathbf{w}_{2j}^\top \mathbf{t}_2(\mathbf{x}) + b_i + b_j) \cdot \frac{\prod_{l=1}^L \Gamma(1 + w_{1il} + w_{1jl})}{\Gamma(L + \sum_{l=1}^L (w_{1il} + w_{1jl}))}, \quad (10)$$

where w_{1il} is the il -th element of matrix \mathbf{W}_1 and $\Gamma(\cdot)$ is the gamma function.

The proof is provided in the Appendix. With the closed-form kernel function in Eq. (10), we can construct the conditional SNEFY distribution $P(d\boldsymbol{\ell}|\mathbf{x}; \mathbf{V}, \boldsymbol{\Theta})$ in the form of Eq. (7). This model provides us with the freedom to choose any sufficient statistic $\mathbf{t}_2(\cdot)$ that is used to transform the input sample \mathbf{x} from the original d -dimensional space to the latent D_2 -dimensional space. To capture the non-linearity between input samples and their label distributions, deep neural networks can be leveraged to construct $\mathbf{t}_2(\cdot)$. The input can also be extended beyond the vector-format samples to data with special structures, like images, texts and graphs, where we can respectively leverage Convolutional Neural Networks (CNNs) [Venkatesan and Li, 2017], Transformers [Vaswani et al., 2017] and Graph Neural Networks (GNNs) [Kipf and Welling, 2017] to construct $\mathbf{t}_2(\cdot)$ for end-to-end learning.

The conditional distribution formulation $P(d\boldsymbol{\ell}|\mathbf{x}; \mathbf{V}, \boldsymbol{\Theta})$ also provides a closed form of mean, variance and co-variance of the label distribution probabilities conditioned on the input sample \mathbf{x} . About this, we have the following theorem:

Theorem 3. Assuming the label distribution vector $\boldsymbol{\ell}$ follows the SNEFY conditional distribution $P(d\boldsymbol{\ell}|\mathbf{x}; \mathbf{V}, \boldsymbol{\Theta})$ in Eq. (7) with the kernel function $\mathbf{k}_{\sigma, \mathbf{t}_1, \mathbf{t}_2, \mu_1}(\boldsymbol{\theta}_i, \boldsymbol{\theta}_j; \mathbf{x})$ given in Eq. (10), under the setting that $\mathbf{t}_1(\boldsymbol{\ell}) = (\log \ell^{y_1}, \log \ell^{y_2}, \dots, \log \ell^{y_L})$, $\sigma = \exp$, and $\mu_1(d\boldsymbol{\ell}) = d\boldsymbol{\ell}$, as well as the constraint that $\mathbf{W}_1 > -1/2$ elementwise, for the affiliation probability to the r th label $y_r \in \mathcal{Y}$, ℓ^{y_r} , we have its conditional mean $E[\ell^{y_r}|\mathbf{x}]$ as

$$E[\ell^{y_r}|\mathbf{x}] = \frac{\text{vec}(\mathbf{V}^\top \mathbf{V})^\top \text{vec}(\mathbf{K}_{\boldsymbol{\Theta}}(\mathbf{x}) \circ \mathbf{F}^{y_r})}{\text{vec}(\mathbf{V}^\top \mathbf{V})^\top \text{vec}(\mathbf{K}_{\boldsymbol{\Theta}}(\mathbf{x}))}, \quad (11)$$

where \circ denotes Hadamard product, and \mathbf{F}^{y_r} is a $n \times n$ matrix, whose ij th entry is

$$F_{ij}^{y_r} = \frac{1 + w_{1ir} + w_{1jr}}{L + \sum_{l=1}^L (w_{1il} + w_{1jl})}. \quad (12)$$

The conditional variance of ℓ^{y_r} , $\text{Var}[\ell^{y_r}|\mathbf{x}]$, is

$$\text{Var}[\ell^{y_r}|\mathbf{x}] = \frac{\text{vec}(\mathbf{V}^\top \mathbf{V})^\top \text{vec}(\mathbf{K}_\Theta(\mathbf{x}) \circ \mathbf{G}^{y_r})}{\text{vec}(\mathbf{V}^\top \mathbf{V})^\top \text{vec}(\mathbf{K}_\Theta(\mathbf{x}))} - \mathbb{E}^2[\ell^{y_r}|\mathbf{x}], \quad (13)$$

where \mathbf{G}^{y_r} is a $n \times n$ matrix, with its ij th element being

$$G_{ij}^{y_r} = \frac{(1 + w_{1ir} + w_{1jr})(2 + w_{1ir} + w_{1jr})}{[L + \sum_{l=1}^L (w_{1il} + w_{1jl})][1 + L + \sum_{l=1}^L (w_{1il} + w_{1jl})]}. \quad (14)$$

For two different labels y_r and y_s , with $y_r \neq y_s$, the conditional covariance of ℓ^{y_r} and ℓ^{y_s} , $\text{Cov}[\ell^{y_r}, \ell^{y_s}|\mathbf{x}]$, is

$$\text{Cov}[\ell^{y_r}, \ell^{y_s}|\mathbf{x}] = \frac{\text{vec}(\mathbf{V}^\top \mathbf{V})^\top \text{vec}(\mathbf{K}_\Theta(\mathbf{x}) \circ \mathbf{H}^{y_r, y_s})}{\text{vec}(\mathbf{V}^\top \mathbf{V})^\top \text{vec}(\mathbf{K}_\Theta(\mathbf{x}))} - \mathbb{E}[\ell^{y_r}|\mathbf{x}] \cdot \mathbb{E}[\ell^{y_s}|\mathbf{x}], \quad (15)$$

where \mathbf{H}^{y_r, y_s} is a $n \times n$ matrix, with its ij th element being

$$H_{ij}^{y_r, y_s} = \frac{(1 + w_{1ir} + w_{1jr})(1 + w_{1is} + w_{1js})}{[L + \sum_{l=1}^L (w_{1il} + w_{1jl})][1 + L + \sum_{l=1}^L (w_{1il} + w_{1jl})]}. \quad (16)$$

The proof is provided in the Appendix. Given the fitted distribution $P(d\ell|\mathbf{x}; \mathbf{V}, \Theta)$, the mean $\mathbb{E}[\ell^{y_r}|\mathbf{x}]$ can be used to predict the unknown label distribution as the expectation over all values in the simplex. We can use the variance $\text{Var}[\ell^{y_r}|\mathbf{x}]$ to quantify label distribution prediction uncertainties. We can also use $\mathbb{E}[\ell^{y_r}|\mathbf{x}]$ with $\text{Var}[\ell^{y_r}|\mathbf{x}]$ to construct confidence intervals for label distribution predictions by applying Chebyshev's inequality [Grimmett and Stirzaker, 2020]. The covariance $\text{Cov}[\ell^{y_r}, \ell^{y_s}|\mathbf{x}]$ is helpful for us to understand the correlations between two different labels. More importantly, all the statistics are conditioned on the input sample \mathbf{x} , guiding us to make instance-wise inferences.

The conditional distribution $P(d\ell|\mathbf{x}; \mathbf{V}, \Theta)$ relies on the parameters \mathbf{V} and Θ , as well as the neural network parameters for constructing \mathbf{t}_2 (we also use \mathbf{t}_2 to denote the parameters without confusion). We train the model with maximum likelihood estimation (MLE), by minimizing the negative log conditional likelihoods on training samples:

$$\min_{\mathbf{V}, \Theta, \mathbf{t}_2} - \sum_{\mathbf{x}' \in \mathcal{X}} \log \left. \frac{P(d\ell|\mathbf{x}; \mathbf{V}, \Theta)}{d\ell} \right|_{\mathbf{x}=\mathbf{x}', \ell=\ell_{\mathbf{x}'}}. \quad (17)$$

There are numerous metrics to measure the consistency between two label distributions, like Chebyshev distance, Kullback-Leibler divergence and Cosine coefficient [Geng, 2016]. Instead of optimizing these metrics, the MLE based learning objective in Eq. (17) provides

Algorithm 1 Training SNEFY-LDL

Input: Training set $\{(\mathbf{x}_1, \ell_{\mathbf{x}_1}), (\mathbf{x}_2, \ell_{\mathbf{x}_2}), \dots, (\mathbf{x}_N, \ell_{\mathbf{x}_N})\}$.

Parameter: $(\mathbf{V}, \Theta, \mathbf{t}_2)$.

Output: Optimized $(\mathbf{V}, \Theta, \mathbf{t}_2)$.

```
1:  $(\mathbf{V}, \Theta, \mathbf{t}_2) \leftarrow$  random initialization;  
2: while epoch number does not expire do  
3:    $\mathcal{B} \leftarrow$  randomly split training set into batches;  
4:   for each batch in  $\mathcal{B}$  do  
5:     Calculate batched  $\mathbf{K}_\Theta(\mathbf{x})$  with Eq. (10);  
6:     Calculate batched likelihoods with Eq. (7);  
7:      $(\mathbf{V}, \Theta, \mathbf{t}_2) \leftarrow$  update by descending along the gradient of batched negative log likelihoods;  
8:   end for  
9: end while  
10: return optimized  $(\mathbf{V}, \Theta, \mathbf{t}_2)$ .
```

an alternative way to train the LDL model. The fitted distribution $P(d\ell|\mathbf{x}; \mathbf{V}, \Theta)$ can be applied to various downstream tasks, and its closed-form mean is able to offer accurate label distribution predictions that are generic to varying evaluation metrics.

Algorithm Description and Time Complexity We train the SNEFY-LDL model with stochastic gradient descent. The training procedure is shown in Algorithm 1. The model parameters \mathbf{V} , Θ and \mathbf{t}_2 are first initialized by random numbers. We then iteratively select a batch of training samples, calculate the batched likelihoods with Eq. (7), and update parameters \mathbf{V} , Θ and \mathbf{t}_2 by descending them along the gradient of batched negative log likelihoods. Taking the epoch number as a constant and assuming the latent layers of \mathbf{t}_2 have neurons in the same scale as the neuron number in the last layer D_2 , the time complexity of Algorithm 1 is $\mathcal{O}(N(mn^2 + Ln^2 + dD_2 + D_2^2))$, which is linear to the number of training samples N , making the algorithm able to scale to large datasets. For any sample \mathbf{x} with an unknown label distribution, its label distribution can be predicted fast in time complexity $\mathcal{O}(mn^2 + Ln^2 + dD_2 + D_2^2)$ using the closed-form mean formulation in Eq. (11).

6 Experiments

In this section, extensive experiments are carried out to evaluate SNEFY-LDL’s performance in label distribution prediction and prediction uncertainty quantification.

Benchmark Datasets We use fourteen datasets [Geng, 2016] to benchmark our experiments, including the *Movie* dataset containing label distributions on five movie rating scales (from one to five), the *Natural Scene* dataset with label distributions constructed by inconsistent multi-label ranking on natural scene images, the facial expression datasets *SBU_3DFE* and *SJAFFE* with label distributions on six emotions, as well as the ten *Yeast* series datasets built from ten biological experiments on a budding yeast, where labels are defined by different time points and label distributions are constructed by different gene expression levels at varying time points. The statistics of the fourteen benchmark datasets are summarized in Table 1.

Baseline Methods We compare the proposed SNEFY-LDL model with eight state-of-the-art LDL baselines:

- **PT-SVM** [Geng, 2016] transforms LDL into a multi-class classification problem and uses SVM as the classifier.
- **AA-KNN** [Geng, 2016] adapts KNN from the single-label classification setting to the LDL setting.
- **CPNN** [Geng et al., 2013] uses a neural network to model the feature-label joint distribution.
- **SA-BFGS** [Geng, 2016] applies the maximum entropy model to characterize label distributions.
- **LDLF** [Shen et al., 2017] employs the differentiable decision trees to model label distributions.
- **DF-LDL** [González et al., 2021a] learns label distributions in a decomposition-fusion manner.
- **LDL-SCL** [Jia et al., 2021] considers the label distribution correlations between similar samples.
- **LDL-LRR** [Jia et al., 2023a] preserves the label importance ranking in label distribution modeling.

No.	Dataset	#Examples	#Features	#Labels
1	Movie	7,755	1,869	5
2	Natural Scene	2,000	294	9
3	SBU_3DFE	2,500	243	6
4	SJAFFE	213	243	6
5	Yeast_alpha	2,465	24	18
6	Yeast_cdc	2,465	24	15
7	Yeast_cold	2,465	24	14
8	Yeast_diau	2,465	24	7
9	Yeast_dtt	2,465	24	6
10	Yeast_elu	2,465	24	6
11	Yeast_heat	2,465	24	4
12	Yeast_spo	2,465	24	4
13	Yeast_spo5	2,465	24	3
14	Yeast_spoem	2,465	24	2

Table 1: Summary of the fourteen benchmark datasets.

Experimental Settings Following [Geng, 2016], we use ten-fold cross-validation to evaluate the label distribution prediction performance, by randomly splitting each dataset into ten chunks, and iteratively choosing a chunk as the test set and taking the remaining nine chunks as the training set. LDL models are then trained on the training set and evaluated on the test set for ten rounds. Averaged performance is used to compare SNEFY-LDL with baseline methods.

The closed-form mean in Eq. (11) is used to make comparisons on the label distribution prediction task with the baselines which all return point estimates on the simplex. However, we note that SNEFY-LDL is a full conditional density model and its utility is broader than the baselines, as we illustrate in the active learning and ensemble learning experiments. When implementing SNEFY-LDL, m and n are respectively set to 32 and 64, D_2 is set as equal to n and a one-layer neural network with ReLU activation is used to construct \mathbf{t}_2 . The model is trained for 100 epochs with batch size 16. Weight clipping [Arjovsky et al., 2017] is used to control $\mathbf{W}_1 > -1/2$ after each parameter update. For the eight baseline models, we use the implementations in the PyLDL library¹ and keep the default hyperparameters.

Evaluation Metrics Following [Geng, 2016], we adopt six metrics to evaluate label distribution prediction performance: Chebyshev distance (Cheby), Clark distance (Clark), Canberra metric (Canb), Kullback-Leibler divergence (KL), Cosine coefficient (Cos) and Intersection (Inter). By denoting ℓ and $\hat{\ell}$ as ground-truth and predicted label distribution vectors

¹<https://github.com/SpriteMisaka/PyLDL>

Dataset	PT-SVM	AA-KNN	CPNN	SA-BFGS	LDLF	DF-LDL	LDL-SCL	LDL-LRR	SNEFY-LDL	Δ
Movie	0.9332 ●	0.9279 ●	0.9244 ●	0.9339 ●	0.8596 ●	0.9357 ♣	0.9036 ●	0.9353 ♣	<u>0.9354</u>	-0.0002
Natural_Scene	0.7404 ♣	0.7112 ●	0.6249 ●	0.7168 ●	0.7304 ♣	0.7377 ♣	0.6716 ●	<u>0.7455</u> ♣	0.7524	+0.0068
SBU_3DFE	0.9244 ●	0.9215 ●	0.9169 ●	0.9383 ●	0.9359 ●	<u>0.9386</u> ●	0.9249 ●	0.9284 ●	0.9427	+0.0042
SJAFFE	0.9336 ●	0.9490 ♣	0.9302 ●	0.9543 ♣	0.9593 ○	0.9646 ○	0.9604 ○	<u>0.9635</u> ○	0.9507	-0.0140
Yeast_alpha	0.9941 ●	0.9938 ●	0.9940 ●	<u>0.9946</u> ○	0.9943 ♣	0.9946 ○	0.9945 ○	0.9946 ○	0.9943	-0.0004
Yeast_cdc	0.9928 ●	0.9924 ●	0.9927 ●	<u>0.9933</u> ○	0.9932 ○	0.9933 ○	0.9932 ○	0.9933 ○	0.9929	-0.0004
Yeast_cold	0.9879 ●	0.9872 ●	0.9875 ●	<u>0.9885</u> ○	0.9876 ●	0.9884 ♣	0.9871 ●	0.9885 ○	0.9883	-0.0002
Yeast_diau	0.9870 ●	0.9867 ●	0.9860 ●	<u>0.9879</u> ○	0.9873 ♣	0.9879 ○	0.9849 ●	0.9879 ○	0.9873	-0.0006
Yeast_dtt	0.9934 ●	0.9934 ●	0.9938 ♣	0.9941 ○	0.9936 ♣	0.9939 ♣	0.9931 ♣	<u>0.9941</u> ○	0.9939	-0.0002
Yeast_elu	0.9933 ●	0.9932 ●	0.9936 ♣	<u>0.9940</u> ○	0.9939 ○	0.9941 ○	0.9939 ○	0.9940 ○	0.9936	-0.0005
Yeast_heat	0.9871 ●	0.9867 ●	0.9874 ●	0.9880 ○	0.9877 ♣	0.9881 ○	0.9873 ♣	<u>0.9880</u> ○	0.9878	-0.0003
Yeast_spo	0.9765 ♣	0.9728 ●	0.9759 ●	<u>0.9770</u> ○	0.9746 ●	0.9756 ●	0.9759 ●	0.9770 ○	0.9766	-0.0004
Yeast_spo5	0.9736 ●	0.9711 ●	0.9737 ●	0.9742 ♣	0.9690 ●	0.9698 ●	0.9640 ●	<u>0.9742</u> ♣	0.9744	+0.0002
Yeast_spoem	0.9783 ●	0.9764 ●	0.9789 ♣	0.9790 ♣	0.9750 ●	0.9694 ●	0.8925 ●	<u>0.9790</u> ♣	0.9792	+0.0001

Table 2: The comparison of label distribution prediction performance measured by Cosine coefficient \uparrow .

respectively, these metrics are defined as follows:

- Cheby($\ell, \hat{\ell}$) = $\|\ell - \hat{\ell}\|_{\infty} \downarrow$.
- Clark($\ell, \hat{\ell}$) = $\left\| \frac{\ell - \hat{\ell}}{\ell + \hat{\ell}} \right\|_2 \downarrow$.
- Canb($\ell, \hat{\ell}$) = $\left\| \frac{\ell - \hat{\ell}}{\ell + \hat{\ell}} \right\|_1 \downarrow$.
- KL($\ell, \hat{\ell}$) = $\sum_{y \in \mathcal{Y}} \ell^y \log \frac{\ell^y}{\hat{\ell}^y} \downarrow$.
- Cos($\ell, \hat{\ell}$) = $\frac{\ell^T \hat{\ell}}{\|\ell\|_2 \|\hat{\ell}\|_2} \uparrow$.
- Inter($\ell, \hat{\ell}$) = $\sum_{y \in \mathcal{Y}} \min(\ell^y, \hat{\ell}^y) \uparrow$.

For each metric, \uparrow (\downarrow) indicates that higher (lower) scores imply better label distribution prediction performance.

Label Distribution Prediction Table 2 shows the label distribution prediction performance measured by Cosine coefficient, as the averaged scores on ten-fold cross-validation. On each dataset, the best performer and runner-up are respectively highlighted by **bold-face** and underline. We perform paired t tests between the proposed SNEFY-LDL and every baseline method, and use symbols ●, ○ and ♣ to respectively denote that SNEFY-LDL is superior, inferior and equivalent to the baseline at 0.05 significance level. The last column Δ gives the performance difference between SNEFY-LDL and the best baseline.

From Table 2, we can find that the proposed SNEFY-LDL achieves very competitive label distribution prediction performance, compared with the state-of-the-art baselines. In

Method	Cheby ↓	Clark ↓	Canb ↓	KL ↓	Cos ↑	Inter ↑
Random	0.1490±0.0098 •	0.6359±0.0247 •	1.1999±0.0448 •	0.1409±0.0136 •	0.9054±0.0093 •	0.7950±0.0089 •
Kmeans	0.1456±0.0076 •	0.6242±0.0176 •	1.1815±0.0320 •	0.1361±0.0072 •	0.9079±0.0068 •	0.7981±0.0077 •
CoreSet	0.1484±0.0164 •	0.6322±0.0383 •	1.1962±0.0720 •	0.1399±0.0179 •	0.9042±0.0158 •	0.7941±0.0171 •
Graph Density	0.1428±0.0059 •	0.6175±0.0197 •	1.1671±0.0346 •	0.1326±0.0068 •	0.9108±0.0057 •	0.8013±0.0076 •
Dirichlet	0.1472±0.0090 •	0.6282±0.0245 •	1.1899±0.0470 •	0.1376±0.0116 •	0.9064±0.0085 •	0.7959±0.0099 •
SNEFY	0.1350±0.0030	0.5981±0.0134	1.1283±0.0254	0.1209±0.0049	0.9191±0.0030	0.8098±0.0042

Table 3: The label distribution active learning performance on the *Movie* dataset.

the majority of cases, the performance of SNEFY-LDL is no worse than the compared baselines. On four datasets, SNEFY-LDL achieves the best Cosine coefficient scores. While SNEFY-LDL does not perform best on the remaining datasets, its performance gap with regard to the best performer is very marginal and even negligible. The performance scores measured by the remaining five metrics are provided in the Appendix, which show the same trend. The competitive label distribution prediction performance implies that the proposed SNEFY-LDL model is able to accurately model the distribution of label distribution vectors, offering an effective tool for label distribution prediction.

Label Distribution Active Learning In addition, we conduct experiments on label distribution active learning to evaluate SNEFY-LDL’s performance in uncertainty quantification. We choose the *Movie* dataset, randomly select 400 labeled training samples to form the initial labeled pool and take the remaining training samples as the unlabeled pool on each fold of cross-validation. The SNEFY-LDL model is first trained on the initial labeled pool. We then use different active learning strategies to pick up 200 informative samples from the unlabeled pool and query their labels. After augmenting the initial labeled pool with the 200 queried samples, we re-train the SNEFY-LDL model and evaluate its label distribution prediction performance on the test sets. Six different active learning strategies are compared:

- **Random** [Zhan et al., 2022] randomly selects 200 samples from the unlabeled pool.
- **Kmeans** [Zhdanov, 2019] selects samples close to the cluster centroids generated by the Kmeans clustering [MacKay, 2003] in feature space.
- **CoreSet** [Sener and Savarese, 2018] selects the k -center samples [Har-Peled, 2011] as representative unlabeled samples, which is a variant of Kmeans.
- **Graph Density** [Ebert et al., 2012] selects highly connected samples in the constructed KNN graph [Preparata and Shamos, 2012].

Base Learner	Bagging	Cheby ↓	Clark ↓	Canb ↓	KL ↓	Cos ↑	Inter ↑
SA-BFGS	Average	0.1178±0.0020●	0.3743±0.0068●	0.7948±0.0163●	0.0641±0.0022●	0.9370±0.0020●	0.8575±0.0028●
	Weighted	0.1137±0.0023	0.3625±0.0062	0.7686±0.0149	0.0604±0.0021	0.9406±0.0020	0.8624±0.0026
DF-LDL	Average	0.1203±0.0017●	0.3762±0.0059●	0.8040±0.0146●	0.0657±0.0019●	0.9353±0.0018●	0.8557±0.0025●
	Weighted	0.1152±0.0024	0.3617±0.0070	0.7715±0.0168	0.0609±0.0024	0.9399±0.0023	0.8617±0.0030
LDL-SCL	Average	0.1256±0.0020●	0.3828±0.0047●	0.8260±0.0118●	0.0699±0.0021●	0.9315±0.0018●	0.8519±0.0020●
	Weighted	0.1246±0.0023	0.3772±0.0048	0.8147±0.0114	0.0684±0.0022	0.9330±0.0019	0.8540±0.0020
LDL-LRR	Average	0.1269±0.0021●	0.3966±0.0052●	0.8478±0.0131●	0.0730±0.0022●	0.9285±0.0019●	0.8478±0.0023●
	Weighted	0.1250±0.0020	0.3916±0.0044	0.8373±0.0106	0.0710±0.0020	0.9305±0.0018	0.8498±0.0019

Table 4: The label distribution ensemble learning performance on the *SBU_3DFE* dataset.

- **Dirichlet** models the distribution of label distributions using a Dirichlet distribution [Ng et al., 2011] centered at predicted label distributions and selects samples with the largest differential entropies [Cover, 1999].
- **SNEFY-LDL** uses importance sampling [Kloek and Van Dijk, 1978] to estimate differential entropies of the conditional distributions modeled by SNEFY-LDL and picks up samples having the largest differential entropies.

Among the six active learning strategies, Kmeans, CoreSet and Graph Density are representativeness based methods, which rely on only sample features by characterizing samples’ geometric properties in feature space, while Dirichlet and SNEFY-LDL are the uncertainty based methods we have contrived, which leverage the predictions of the initially trained SNEFY-LDL model.

Table 3 shows the performance of different active learning strategies, where the best performer is highlighted by **boldface** and ● indicates that the annotated performer is inferior to the best performer at 0.05 significance level. As is shown in Table 3, SNEFY-LDL consistently achieves the best performance in terms of all metrics. By accurately evaluating label distribution prediction uncertainties, SNEFY-LDL can pick up more informative unlabeled samples than the naive uncertainty quantification strategy, Dirichlet, as well as the representativeness based active learning strategies, Kmeans, CoreSet and Graph Density, which are even sometimes inferior to the Random strategy.

Label Distribution Ensemble Learning We also conduct experiments on ensemble learning to further verify SNEFY-LDL’s ability in uncertainty quantification, by using Bagging [Breiman, 1996] as an exemplary ensemble learning paradigm. We choose the *SBU_3DFE* dataset, randomly select 50 samples from the training split of each fold of cross-validation for 25 rounds, train 25 base LDL learners with the selected samples, and evaluate the label distribution prediction performance of ensembled LDL models on the test sets. Four

competitive LDL models are employed as base learners: SA-BFGS, DF-LDL, LDL-SCL and LDL-LRR, and two strategies are adopted to ensemble base learner predictions: 1) **Average**: aggregate the 25 base learner predictions with the uniform weight $1/25$, and 2) **Weighted**: weight each base learner prediction in proportion to its SNEFY-LDL conditional likelihood in an instance-wise manner.

Table 4 compares the two different ensemble learning strategies, where the best strategy is highlighted by **boldface** and **•** indicates that the annotated strategy is inferior to the best strategy at 0.05 significance level. From Table 4, we can find that the **Weighted** strategy is significantly better than **Average** in terms of all metrics. This implies that SNEFY-LDL provides an effective mechanism to quantify the prediction reliability/uncertainties of base learners.

Parameter Sensitivity Study We also conduct additional experiments to investigate SNEFY-LDL’s sensitivity with regard to its four hyperparameters: n and m , as well as the batch size and epoch number used for training. The experiments demonstrate that the performance of SNEFY-LDL remains relatively stable when the hyperparameters vary in proper ranges. Please check the Appendix for more details.

7 Conclusion

In this paper, we propose a novel LDL paradigm: estimate the distribution of label distribution vectors in the probability simplex, which brings a bird’s-eye view on the relative significance of all possible label distributions. Through uncovering the underlying relationship between SNEFY and LDL, we develop the SNEFY-LDL model that can provide a tractable formulation of the conditional distribution of label distribution vectors, enjoying great expressivity and high computational efficiency. SNEFY-LDL admits closed-form expressions for the distribution’s mean, variance and covariance that can be computed quickly, making SNEFY-LDL able to provide real-time responses to the downstream tasks and real-world applications. Experiments on label distribution prediction, as well as label distribution active learning and ensemble learning demonstrate the great utility of SNEFY-LDL for label distribution modeling.

References

Martin Arjovsky, Soumith Chintala, and Léon Bottou. Wasserstein generative adversarial networks. In *International Conference on Machine Learning*, pages 214–223. PMLR, 2017.

- Leo Breiman. Bagging predictors. *Machine learning*, 24:123–140, 1996.
- Shikai Chen, Jianfeng Wang, Yuedong Chen, Zhongchao Shi, Xin Geng, and Yong Rui. Label distribution learning on auxiliary label space graphs for facial expression recognition. In *Proceedings of the IEEE/CVF Conference on Computer Vision and Pattern Recognition*, pages 13984–13993, 2020.
- Thomas M Cover. *Elements of information theory*. John Wiley & Sons, 1999.
- Sandra Ebert, Mario Fritz, and Bernt Schiele. Ralf: A reinforced active learning formulation for object class recognition. In *2012 IEEE Conference on Computer Vision and Pattern Recognition*, pages 3626–3633. IEEE, 2012.
- Xin Geng. Label distribution learning. *IEEE Transactions on Knowledge and Data Engineering*, 28(7):1734–1748, 2016.
- Xin Geng and Peng Hou. Pre-release prediction of crowd opinion on movies by label distribution learning. In *International Joint Conference on Artificial Intelligence*, pages 3511–3517. Citeseer, 2015.
- Xin Geng, Chao Yin, and Zhi-Hua Zhou. Facial age estimation by learning from label distributions. *IEEE Transactions on Pattern Analysis and Machine Intelligence*, 35(10):2401–2412, 2013.
- Manuel González, Germán González-Almagro, Isaac Triguero, José-Ramón Cano, and Salvador García. Decomposition-fusion for label distribution learning. *Information Fusion*, 66:64–75, 2021a.
- Manuel González, Julián Luengo, José-Ramón Cano, and Salvador García. Synthetic sample generation for label distribution learning. *Information Sciences*, 544:197–213, 2021b.
- Michael Greenacre. Compositional Data Analysis. *Annual Review of Statistics and Its Application*, 8(Volume 8, 2021):271–299, March 2021. ISSN 2326-8298, 2326-831X. doi: 10.1146/annurev-statistics-042720-124436.
- Geoffrey Grimmett and David Stirzaker. *Probability and random processes*. Oxford university press, 2020.
- Sariel Har-Peled. *Geometric approximation algorithms*. Number 173. American Mathematical Soc., 2011.

- Liang He, Yunan Lu, Weiwei Li, and Xiuyi Jia. Generative calibration of inaccurate annotation for label distribution learning. In *Proceedings of the AAAI Conference on Artificial Intelligence*, volume 38, pages 12394–12401, 2024.
- Weiming Huang, Daokun Zhang, Gengchen Mai, Xu Guo, and Lizhen Cui. Learning urban region representations with pois and hierarchical graph infomax. *ISPRS Journal of Photogrammetry and Remote Sensing*, 196:134–145, 2023.
- Xiuyi Jia, Zechao Li, Xiang Zheng, Weiwei Li, and Sheng-Jun Huang. Label distribution learning with label correlations on local samples. *IEEE Transactions on Knowledge and Data Engineering*, 33(4):1619–1631, 2021.
- Xiuyi Jia, Tian Qin, Yunan Lu, and Weiwei Li. Adaptive weighted ranking-oriented label distribution learning. *IEEE Transactions on Neural Networks and Learning Systems*, 2023a.
- Xiuyi Jia, Xiaoxia Shen, Weiwei Li, Yunan Lu, and Jihua Zhu. Label distribution learning by maintaining label ranking relation. *IEEE Transactions on Knowledge and Data Engineering*, 35(2):1695–1707, 2023b.
- Thomas N Kipf and Max Welling. Semi-supervised classification with graph convolutional networks. *International Conference on Learning Representations*, 2017.
- Teun Kloek and Herman K Van Dijk. Bayesian estimates of equation system parameters: an application of integration by monte carlo. *Econometrica: Journal of the Econometric Society*, pages 1–19, 1978.
- Peter Kotschieder, Madalina Fiterau, Antonio Criminisi, and Samuel Rota Buló. Deep neural decision forests. In *Proceedings of the IEEE International Conference on Computer Vision*, pages 1467–1475, 2015.
- David JC MacKay. *Information theory, inference and learning algorithms*. Cambridge university press, 2003.
- Robert Malouf. A comparison of algorithms for maximum entropy parameter estimation. In *International Conference on Computational Linguistics*, 2002.
- Dharmendra S Modha and Yeshaiah Fainman. A learning law for density estimation. *IEEE Transactions on Neural Networks*, 5(3):519–523, 1994.

- Kai Wang Ng, Guo-Liang Tian, and Man-Lai Tang. Dirichlet and related distributions: Theory, methods and applications. 2011.
- Jorge Nocedal and Stephen J Wright. *Numerical optimization*. Springer, 1999.
- Franco P Preparata and Michael I Shamos. *Computational geometry: an introduction*. Springer Science & Business Media, 2012.
- Ozan Sener and Silvio Savarese. Active learning for convolutional neural networks: A core-set approach. In *International Conference on Learning Representations*, 2018.
- Wei Shen, Kai Zhao, Yilu Guo, and Alan L Yuille. Label distribution learning forests. *Advances in Neural Information Processing Systems*, 30, 2017.
- Amirreza Shirani, Franck Deroncourt, Paul Asente, Nedim Lipka, Seokhwan Kim, Jose Echevarria, and Tamar Solorio. Learning emphasis selection for written text in visual media from crowd-sourced label distributions. In *Proceedings of the Annual Meeting of the Association for Computational Linguistics*, pages 1167–1172, 2019.
- Russell Tsuchida, Cheng Soon Ong, and Dino Sejdinovic. Squared neural families: a new class of tractable density models. *Advances in Neural Information Processing Systems*, 36, 2023.
- Ashish Vaswani, Noam Shazeer, Niki Parmar, Jakob Uszkoreit, Llion Jones, Aidan N Gomez, Lukasz Kaiser, and Illia Polosukhin. Attention is all you need. *Advances in Neural Information Processing Systems*, 30, 2017.
- Ragav Venkatesan and Baoxin Li. *Convolutional neural networks in visual computing: a concise guide*. CRC Press, 2017.
- Jing Wang and Xin Geng. Classification with label distribution learning. In *International Joint Conference on Artificial Intelligence*, volume 1, page 2, 2019.
- Jing Wang and Xin Geng. Label distribution learning machine. In *International Conference on Machine Learning*, pages 10749–10759. PMLR, 2021a.
- Jing Wang and Xin Geng. Learn the highest label and rest label description degrees. In *International Joint Conference on Artificial Intelligence*, pages 3097–3103, 2021b.
- Changsong Wen, Xin Zhang, Xingxu Yao, and Jufeng Yang. Ordinal label distribution learning. In *Proceedings of the IEEE/CVF International Conference on Computer Vision*, pages 23481–23491, 2023.

- Xiaoping Wu, Ni Wen, Jie Liang, Yu-Kun Lai, Dongyu She, Ming-Ming Cheng, and Jufeng Yang. Joint acne image grading and counting via label distribution learning. In *Proceedings of the IEEE/CVF International Conference on Computer Vision*, pages 10642–10651, 2019.
- Xindong Wu, Vipin Kumar, J Ross Quinlan, Joydeep Ghosh, Qiang Yang, Hiroshi Motoda, Geoffrey J McLachlan, Angus Ng, Bing Liu, Philip S Yu, et al. Top 10 algorithms in data mining. *Knowledge and Information Systems*, 14:1–37, 2008.
- Kouzhiqiang Yucheng Xie, Jing Wang, Yuheng Jia, Boyu Shi, and Xin Geng. Rankmatch: A novel approach to semi-supervised label distribution learning leveraging inter-label correlations. *arXiv preprint arXiv:2312.06343*, 2023.
- Luhui Xu, Jingying Chen, and Yanling Gan. Head pose estimation using improved label distribution learning with fewer annotations. *Multimedia Tools and Applications*, 78: 19141–19162, 2019a.
- Miao Xu and Zhi-Hua Zhou. Incomplete label distribution learning. In *International Joint Conference on Artificial Intelligence*, pages 3175–3181, 2017.
- Ning Xu, Yun-Peng Liu, and Xin Geng. Label enhancement for label distribution learning. *IEEE Transactions on Knowledge and Data Engineering*, 33(4):1632–1643, 2019b.
- Ning Xu, Jun Shu, Yun-Peng Liu, and Xin Geng. Variational label enhancement. In *International Conference on Machine Learning*, pages 10597–10606. PMLR, 2020.
- Jufeng Yang, Ming Sun, and Xiaoxiao Sun. Learning visual sentiment distributions via augmented conditional probability neural network. In *Proceedings of the AAAI Conference on Artificial Intelligence*, volume 31, 2017.
- Xueying Zhan, Qingzhong Wang, Kuan-hao Huang, Haoyi Xiong, Dejing Dou, and Antoni B Chan. A comparative survey of deep active learning. *arXiv preprint arXiv:2203.13450*, 2022.
- Fedor Zhdanov. Diverse mini-batch active learning. *arXiv preprint arXiv:1901.05954*, 2019.
- Qinghai Zheng, Jihua Zhu, and Haoyu Tang. Label information bottleneck for label enhancement. In *Proceedings of the IEEE/CVF Conference on Computer Vision and Pattern Recognition*, pages 7497–7506, 2023.

Appendices

A Theorem Proofs

Theorem 2. Let $\mathbf{t}_1(\boldsymbol{\ell}) = (\log \ell^{y_1}, \log \ell^{y_2}, \dots, \log \ell^{y_L}) : \Delta^{L-1} \rightarrow \mathbb{R}^L$ by setting $D_1 = L$, the activation function σ be the exponential function \exp , the base measure $\mu_1(d\boldsymbol{\ell}) = d\boldsymbol{\ell}$ be the Lebesgue measure. Under the condition that $\mathbf{W}_1 > -1/2$ elementwise, the kernel function $\mathbf{k}_{\sigma, \mathbf{t}_1, \mathbf{t}_2, \mu_1}(\boldsymbol{\theta}_i, \boldsymbol{\theta}_j; \mathbf{x})$ admits a closed form:

$$\mathbf{k}_{\mathbf{t}_2}(\boldsymbol{\theta}_i, \boldsymbol{\theta}_j; \mathbf{x}) = \exp(\mathbf{w}_{2i}^\top \mathbf{t}_2(\mathbf{x}) + \mathbf{w}_{2j}^\top \mathbf{t}_2(\mathbf{x}) + b_i + b_j) \cdot \frac{\prod_{l=1}^L \Gamma(1 + w_{1il} + w_{1jl})}{\Gamma(L + \sum_{l=1}^L (w_{1il} + w_{1jl}))}, \quad (10)$$

where w_{1il} is the il -th element of matrix \mathbf{W}_1 and $\Gamma(\cdot)$ is the gamma function.

Proof. According to Eq. (9),

$$\begin{aligned} \mathbf{k}_{\sigma, \mathbf{t}_1, \mathbf{t}_2, \mu_1}(\boldsymbol{\theta}_i, \boldsymbol{\theta}_j; \mathbf{x}) &= \int_{\Delta^{L-1}} \tilde{\mathbf{k}}_{\sigma, \mathbf{t}_1, \mathbf{t}_2}(\boldsymbol{\theta}_i, \boldsymbol{\theta}_j; \boldsymbol{\ell}, \mathbf{x}) \mu_1(d\boldsymbol{\ell}) \\ &= \int_{\Delta^{L-1}} \sigma(\mathbf{w}_{1i}^\top \mathbf{t}_1(\boldsymbol{\ell}) + \mathbf{w}_{2i}^\top \mathbf{t}_2(\mathbf{x}) + b_i) \cdot \sigma(\mathbf{w}_{1j}^\top \mathbf{t}_1(\boldsymbol{\ell}) + \mathbf{w}_{2j}^\top \mathbf{t}_2(\mathbf{x}) + b_j) \mu_1(d\boldsymbol{\ell}). \end{aligned}$$

Given the setting $\mathbf{t}_1(\boldsymbol{\ell}) = (\log \ell^{y_1}, \log \ell^{y_2}, \dots, \log \ell^{y_L})$, $\sigma = \exp$ and $\mu_1(d\boldsymbol{\ell}) = d\boldsymbol{\ell}$, $\mathbf{k}_{\sigma, \mathbf{t}_1, \mathbf{t}_2, \mu_1}$ can be written as

$$\begin{aligned} \mathbf{k}_{\mathbf{t}_2}(\boldsymbol{\theta}_i, \boldsymbol{\theta}_j; \mathbf{x}) &= \int_{\Delta^{L-1}} \exp(\mathbf{w}_{1i}^\top \mathbf{t}_1(\boldsymbol{\ell}) + \mathbf{w}_{2i}^\top \mathbf{t}_2(\mathbf{x}) + b_i) \cdot \exp(\mathbf{w}_{1j}^\top \mathbf{t}_1(\boldsymbol{\ell}) + \mathbf{w}_{2j}^\top \mathbf{t}_2(\mathbf{x}) + b_j) d\boldsymbol{\ell} \\ &= \exp(\mathbf{w}_{2i}^\top \mathbf{t}_2(\mathbf{x}) + \mathbf{w}_{2j}^\top \mathbf{t}_2(\mathbf{x}) + b_i + b_j) \cdot \int_{\Delta^{L-1}} \prod_{l=1}^L (\ell^{y_l})^{w_{1il} + w_{1jl}} d\boldsymbol{\ell}. \end{aligned}$$

As $\mathbf{W}_1 > -1/2$ elementwise, $w_{1il} + w_{1jl} + 1 > 0$. Assuming $\boldsymbol{\ell}$ follows a Dirichlet distribution (Ng, Tian, and Tang 2011) with parameters $\boldsymbol{\alpha} = (\alpha_1, \alpha_2, \dots, \alpha_L)$, where $\alpha_l = w_{1il} + w_{1jl} + 1 > 0$, its probability density, $P_{\text{Dir}}(d\boldsymbol{\ell})/d\boldsymbol{\ell}$, is in the form:

$$\frac{P_{\text{Dir}}(d\boldsymbol{\ell})}{d\boldsymbol{\ell}} = \frac{1}{B(\boldsymbol{\alpha})} \prod_{l=1}^L (\ell^{y_l})^{\alpha_l - 1},$$

where $B(\cdot)$ is the beta function. Considering the fact that $\int_{\Delta^{L-1}} P_{\text{Dir}}(d\boldsymbol{\ell}) = 1$,

$$\int_{\Delta^{L-1}} \prod_{l=1}^L (\ell^{y_l})^{\alpha_l - 1} d\boldsymbol{\ell} = B(\boldsymbol{\alpha}).$$

That is to say

$$\int_{\Delta^{L-1}} \prod_{l=1}^L (\ell^{y_l})^{w_{1il}+w_{1jl}} d\boldsymbol{\ell} = \frac{\prod_{l=1}^L \Gamma(1 + w_{1il} + w_{1jl})}{\Gamma(L + \sum_{l=1}^L (w_{1il} + w_{1jl}))}.$$

Therefore,

$$\mathbf{k}_{\mathbf{t}_2}(\boldsymbol{\theta}_i, \boldsymbol{\theta}_j; \mathbf{x}) = \exp(\mathbf{w}_{2i}^\top \mathbf{t}_2(\mathbf{x}) + \mathbf{w}_{2j}^\top \mathbf{t}_2(\mathbf{x}) + b_i + b_j) \cdot \frac{\prod_{l=1}^L \Gamma(1 + w_{1il} + w_{1jl})}{\Gamma(L + \sum_{l=1}^L (w_{1il} + w_{1jl}))}.$$

□

Theorem 3. Assuming the label distribution vector $\boldsymbol{\ell}$ follows the SNEFY conditional distribution $P(d\boldsymbol{\ell}|\mathbf{x}; \mathbf{V}, \boldsymbol{\Theta})$ in Eq. (7) with the kernel function $\mathbf{k}_{\sigma, \mathbf{t}_1, \mathbf{t}_2, \mu_1}(\boldsymbol{\theta}_i, \boldsymbol{\theta}_j; \mathbf{x})$ given in Eq. (10), under the setting that $\mathbf{t}_1(\boldsymbol{\ell}) = (\log \ell^{y_1}, \log \ell^{y_2}, \dots, \log \ell^{y_L})$, $\sigma = \exp$, and $\mu_1(d\boldsymbol{\ell}) = d\boldsymbol{\ell}$, as well as the constraint that $\mathbf{W}_1 > -1/2$ elementwise, for the affiliation probability to the r th label $y_r \in \mathcal{Y}$, ℓ^{y_r} , we have its conditional mean $E[\ell^{y_r}|\mathbf{x}]$ as

$$E[\ell^{y_r}|\mathbf{x}] = \frac{\text{vec}(\mathbf{V}^\top \mathbf{V})^\top \text{vec}(\mathbf{K}_{\boldsymbol{\Theta}}(\mathbf{x}) \circ \mathbf{F}^{y_r})}{\text{vec}(\mathbf{V}^\top \mathbf{V})^\top \text{vec}(\mathbf{K}_{\boldsymbol{\Theta}}(\mathbf{x}))}, \quad (11)$$

where \circ denotes Hadamard product, and \mathbf{F}^{y_r} is a $n \times n$ matrix, whose ij th entry is

$$F_{ij}^{y_r} = \frac{1 + w_{1ir} + w_{1jr}}{L + \sum_{l=1}^L (w_{1il} + w_{1jl})}. \quad (12)$$

The conditional variance of ℓ^{y_r} , $\text{Var}[\ell^{y_r}|\mathbf{x}]$, is

$$\text{Var}[\ell^{y_r}|\mathbf{x}] = \frac{\text{vec}(\mathbf{V}^\top \mathbf{V})^\top \text{vec}(\mathbf{K}_{\boldsymbol{\Theta}}(\mathbf{x}) \circ \mathbf{G}^{y_r})}{\text{vec}(\mathbf{V}^\top \mathbf{V})^\top \text{vec}(\mathbf{K}_{\boldsymbol{\Theta}}(\mathbf{x}))} - E^2[\ell^{y_r}|\mathbf{x}], \quad (13)$$

where \mathbf{G}^{y_r} is a $n \times n$ matrix, with its ij th element being

$$G_{ij}^{y_r} = \frac{(1 + w_{1ir} + w_{1jr})(2 + w_{1ir} + w_{1jr})}{[L + \sum_{l=1}^L (w_{1il} + w_{1jl})][1 + L + \sum_{l=1}^L (w_{1il} + w_{1jl})]}. \quad (14)$$

For two different labels y_r and y_s , with $y_r \neq y_s$, the conditional covariance of ℓ^{y_r} and ℓ^{y_s} , $\text{Cov}[\ell^{y_r}, \ell^{y_s}|\mathbf{x}]$, is

$$\text{Cov}[\ell^{y_r}, \ell^{y_s}|\mathbf{x}] = \frac{\text{vec}(\mathbf{V}^\top \mathbf{V})^\top \text{vec}(\mathbf{K}_{\boldsymbol{\Theta}}(\mathbf{x}) \circ \mathbf{H}^{y_r, y_s})}{\text{vec}(\mathbf{V}^\top \mathbf{V})^\top \text{vec}(\mathbf{K}_{\boldsymbol{\Theta}}(\mathbf{x}))} - E[\ell^{y_r}|\mathbf{x}] \cdot E[\ell^{y_s}|\mathbf{x}], \quad (15)$$

where \mathbf{H}^{y_r, y_s} is a $n \times n$ matrix, with its ij th element being

$$H_{ij}^{y_r, y_s} = \frac{(1 + w_{1ir} + w_{1jr})(1 + w_{1is} + w_{1js})}{[L + \sum_{l=1}^L (w_{1il} + w_{1jl})][1 + L + \sum_{l=1}^L (w_{1il} + w_{1jl})]}. \quad (16)$$

Proof. For any fixed function $\varphi(\boldsymbol{\ell})$ of $\boldsymbol{\ell}$, its expectation with regard to the conditional SNEFY distribution in Eq. (7), $E[\varphi(\boldsymbol{\ell})|\mathbf{x}]$, can be computed as

$$\begin{aligned} E[\varphi(\boldsymbol{\ell})|\mathbf{x}] &= \int_{\Delta^{L-1}} \varphi(\boldsymbol{\ell}) P(d\boldsymbol{\ell}|\mathbf{x}; \mathbf{V}, \boldsymbol{\Theta}) \\ &= \int_{\Delta^{L-1}} \varphi(\boldsymbol{\ell}) \frac{\text{vec}(\mathbf{V}^\top \mathbf{V})^\top \text{vec}(\widetilde{\mathbf{K}}_{\boldsymbol{\Theta}}(\boldsymbol{\ell}, \mathbf{x}))}{\text{vec}(\mathbf{V}^\top \mathbf{V})^\top \text{vec}(\mathbf{K}_{\boldsymbol{\Theta}}(\mathbf{x}))} \mu_1(d\boldsymbol{\ell}) \\ &= \frac{\text{vec}(\mathbf{V}^\top \mathbf{V})^\top \text{vec}(\boldsymbol{\Phi}_{\boldsymbol{\Theta}}(\mathbf{x}))}{\text{vec}(\mathbf{V}^\top \mathbf{V})^\top \text{vec}(\mathbf{K}_{\boldsymbol{\Theta}}(\mathbf{x}))}, \end{aligned}$$

where $\boldsymbol{\Phi}_{\boldsymbol{\Theta}}(\mathbf{x}) \in \mathbb{R}^{n \times n}$ is the elementwise integral:

$$\boldsymbol{\Phi}_{\boldsymbol{\Theta}}(\mathbf{x}) = \int_{\Delta^{L-1}} \varphi(\boldsymbol{\ell}) \widetilde{\mathbf{K}}_{\boldsymbol{\Theta}}(\boldsymbol{\ell}, \mathbf{x}) \mu_1(d\boldsymbol{\ell}),$$

whose ij th element is

$$\begin{aligned} \phi_{\sigma, \mathbf{t}_1, \mathbf{t}_2, \mu_1}(\boldsymbol{\theta}_i, \boldsymbol{\theta}_j; \mathbf{x}) &= \int_{\Delta^{L-1}} \varphi(\boldsymbol{\ell}) \tilde{\mathbf{k}}_{\sigma, \mathbf{t}_1, \mathbf{t}_2}(\boldsymbol{\theta}_i, \boldsymbol{\theta}_j; \boldsymbol{\ell}, \mathbf{x}) \mu_1(d\boldsymbol{\ell}) \\ &= \int_{\Delta^{L-1}} \varphi(\boldsymbol{\ell}) \sigma(\mathbf{w}_{1i}^\top \mathbf{t}_1(\boldsymbol{\ell}) + \mathbf{w}_{2i}^\top \mathbf{t}_2(\mathbf{x}) + b_i) \cdot \sigma(\mathbf{w}_{1j}^\top \mathbf{t}_1(\boldsymbol{\ell}) + \mathbf{w}_{2j}^\top \mathbf{t}_2(\mathbf{x}) + b_j) \mu_1(d\boldsymbol{\ell}). \end{aligned}$$

By setting $\mathbf{t}_1(\boldsymbol{\ell}) = (\log \boldsymbol{\ell}^{y_1}, \log \boldsymbol{\ell}^{y_2}, \dots, \log \boldsymbol{\ell}^{y_L})$, $\sigma = \exp$, and $\mu_1(d\boldsymbol{\ell}) = d\boldsymbol{\ell}$, $\phi_{\sigma, \mathbf{t}_1, \mathbf{t}_2, \mu_1}(\boldsymbol{\theta}_i, \boldsymbol{\theta}_j; \mathbf{x})$ can be written as

$$\begin{aligned} \phi_{\mathbf{t}_2}(\boldsymbol{\theta}_i, \boldsymbol{\theta}_j; \mathbf{x}) &= \int_{\Delta^{L-1}} \varphi(\boldsymbol{\ell}) \exp(\mathbf{w}_{1i}^\top \mathbf{t}_1(\boldsymbol{\ell}) + \mathbf{w}_{2i}^\top \mathbf{t}_2(\mathbf{x}) + b_i) \cdot \exp(\mathbf{w}_{1j}^\top \mathbf{t}_1(\boldsymbol{\ell}) + \mathbf{w}_{2j}^\top \mathbf{t}_2(\mathbf{x}) + b_j) d\boldsymbol{\ell} \\ &= \exp(\mathbf{w}_{2i}^\top \mathbf{t}_2(\mathbf{x}) + \mathbf{w}_{2j}^\top \mathbf{t}_2(\mathbf{x}) + b_i + b_j) \cdot \int_{\Delta^{L-1}} \varphi(\boldsymbol{\ell}) \prod_{l=1}^L (\boldsymbol{\ell}^{y_l})^{w_{1il} + w_{1jl}} d\boldsymbol{\ell} \end{aligned}$$

As $\mathbf{W}_1 > -1/2$ elementwise, $w_{1il} + w_{1jl} + 1 > 0$. Assuming $\boldsymbol{\ell}$ follows a Dirichlet distribution with parameters $\boldsymbol{\alpha} = (\alpha_1, \alpha_2, \dots, \alpha_L)$, where $\alpha_l = w_{1il} + w_{1jl} + 1 > 0$, its probability density, $P_{\text{Dir}}(d\boldsymbol{\ell})/d\boldsymbol{\ell}$, is in the form:

$$\frac{P_{\text{Dir}}(d\boldsymbol{\ell})}{d\boldsymbol{\ell}} = \frac{1}{\text{B}(\boldsymbol{\alpha})} \prod_{l=1}^L (\boldsymbol{\ell}^{y_l})^{\alpha_l - 1},$$

where $B(\cdot)$ is the beta function. Then, we have

$$\begin{aligned}
\int_{\Delta^{L-1}} \varphi(\boldsymbol{\ell}) \prod_{l=1}^L (\ell^{y_l})^{w_{1il}+w_{1jl}} d\boldsymbol{\ell} &= B(\boldsymbol{\alpha}) \int_{\Delta^{L-1}} \varphi(\boldsymbol{\ell}) P_{\text{Dir}}(d\boldsymbol{\ell}) \\
&= B(\boldsymbol{\alpha}) E_{\text{Dir}}[\varphi(\boldsymbol{\ell}); \mathbf{w}_{1i}, \mathbf{w}_{1j}] \\
&= \frac{\prod_{l=1}^L \Gamma(1 + w_{1il} + w_{1jl})}{\Gamma(L + \sum_{l=1}^L (w_{1il} + w_{1jl}))} E_{\text{Dir}}[\varphi(\boldsymbol{\ell}); \mathbf{w}_{1i}, \mathbf{w}_{1j}],
\end{aligned}$$

where $E_{\text{Dir}}[\varphi(\boldsymbol{\ell}); \mathbf{w}_{1i}, \mathbf{w}_{1j}]$ is the expectation of $\varphi(\boldsymbol{\ell})$ with regard to the Dirichlet distribution parameterized by \mathbf{w}_{1i} and \mathbf{w}_{1j} . Therefore,

$$\begin{aligned}
\phi_{\mathbf{t}_2}(\boldsymbol{\theta}_i, \boldsymbol{\theta}_j; \mathbf{x}) &= \exp(\mathbf{w}_{2i}^\top \mathbf{t}_2(\mathbf{x}) + \mathbf{w}_{2j}^\top \mathbf{t}_2(\mathbf{x}) + b_i + b_j) \\
&\quad \cdot \frac{\prod_{l=1}^L \Gamma(1 + w_{1il} + w_{1jl})}{\Gamma(L + \sum_{l=1}^L (w_{1il} + w_{1jl}))} E_{\text{Dir}}[\varphi(\boldsymbol{\ell}); \mathbf{w}_{1i}, \mathbf{w}_{1j}] \\
&= \mathbf{k}_{\mathbf{t}_2}(\boldsymbol{\theta}_i, \boldsymbol{\theta}_j; \mathbf{x}) E_{\text{Dir}}[\varphi(\boldsymbol{\ell}); \mathbf{w}_{1i}, \mathbf{w}_{1j}].
\end{aligned}$$

By using \mathbf{E}_φ to denote the $n \times n$ matrix whose ij th element is $E_{\text{Dir}}[\varphi(\boldsymbol{\ell}); \mathbf{w}_{1i}, \mathbf{w}_{1j}]$, we have

$$\Phi_{\boldsymbol{\Theta}}(\mathbf{x}) = \mathbf{K}_{\boldsymbol{\Theta}}(\mathbf{x}) \circ \mathbf{E}_\varphi,$$

$$E[\varphi(\boldsymbol{\ell})|\mathbf{x}] = \frac{\text{vec}(\mathbf{V}^\top \mathbf{V})^\top \text{vec}(\mathbf{K}_{\boldsymbol{\Theta}}(\mathbf{x}) \circ \mathbf{E}_\varphi)}{\text{vec}(\mathbf{V}^\top \mathbf{V})^\top \text{vec}(\mathbf{K}_{\boldsymbol{\Theta}}(\mathbf{x}))}.$$

For the Dirichlet distribution, $E_{\text{Dir}}[\varphi(\boldsymbol{\ell}); \mathbf{w}_{1i}, \mathbf{w}_{1j}]$ has closed forms for some moments. In particular, for $\varphi(\boldsymbol{\ell}) = \ell^{y_r}$, $\varphi(\boldsymbol{\ell}) = (\ell^{y_r})^2$, and $\varphi(\boldsymbol{\ell}) = \ell^{y_r} \cdot \ell^{y_s}$ with $y_r \neq y_s$, we respectively have

$$\begin{aligned}
E_{\text{Dir}}[\ell^{y_r}; \mathbf{w}_{1i}, \mathbf{w}_{1j}] &= \frac{1 + w_{1ir} + w_{1jr}}{L + \sum_{l=1}^L (w_{1il} + w_{1jl})}. \\
E_{\text{Dir}}[(\ell^{y_r})^2; \mathbf{w}_{1i}, \mathbf{w}_{1j}] &= \frac{(1 + w_{1ir} + w_{1jr})(2 + w_{1ir} + w_{1jr})}{[L + \sum_{l=1}^L (w_{1il} + w_{1jl})][1 + L + \sum_{l=1}^L (w_{1il} + w_{1jl})]}. \\
E_{\text{Dir}}[\ell^{y_r} \cdot \ell^{y_s}; \mathbf{w}_{1i}, \mathbf{w}_{1j}] &= \frac{(1 + w_{1ir} + w_{1jr})(1 + w_{1is} + w_{1js})}{[L + \sum_{l=1}^L (w_{1il} + w_{1jl})][1 + L + \sum_{l=1}^L (w_{1il} + w_{1jl})]}.
\end{aligned}$$

Finally, we have

$$\begin{aligned} \mathbb{E}[\ell^{y_r}|\mathbf{x}] &= \frac{\text{vec}(\mathbf{V}^\top \mathbf{V})^\top \text{vec}(\mathbf{K}_\Theta(\mathbf{x}) \circ \mathbf{F}^{y_r})}{\text{vec}(\mathbf{V}^\top \mathbf{V})^\top \text{vec}(\mathbf{K}_\Theta(\mathbf{x}))}, \\ \mathbb{E}[(\ell^{y_r})^2|\mathbf{x}] &= \frac{\text{vec}(\mathbf{V}^\top \mathbf{V})^\top \text{vec}(\mathbf{K}_\Theta(\mathbf{x}) \circ \mathbf{G}^{y_r})}{\text{vec}(\mathbf{V}^\top \mathbf{V})^\top \text{vec}(\mathbf{K}_\Theta(\mathbf{x}))}, \\ \mathbb{E}[\ell^{y_r} \cdot \ell^{y_s}|\mathbf{x}] &= \frac{\text{vec}(\mathbf{V}^\top \mathbf{V})^\top \text{vec}(\mathbf{K}_\Theta(\mathbf{x}) \circ \mathbf{H}^{y_r, y_s})}{\text{vec}(\mathbf{V}^\top \mathbf{V})^\top \text{vec}(\mathbf{K}_\Theta(\mathbf{x}))}, \end{aligned}$$

where \mathbf{F}^{y_r} , \mathbf{G}^{y_r} and \mathbf{H}^{y_r, y_s} denote the $n \times n$ matrices whose ij th elements are $\mathbb{E}_{\text{Dir}}[\ell^{y_r}; \mathbf{w}_{1i}, \mathbf{w}_{1j}]$, $\mathbb{E}_{\text{Dir}}[(\ell^{y_r})^2; \mathbf{w}_{1i}, \mathbf{w}_{1j}]$ and $\mathbb{E}_{\text{Dir}}[\ell^{y_r} \cdot \ell^{y_s}; \mathbf{w}_{1i}, \mathbf{w}_{1j}]$ respectively.

$\text{Var}[\ell^{y_r}|\mathbf{x}]$ and $\text{Cov}[\ell^{y_r}, \ell^{y_s}|\mathbf{x}]$ can be directly derived by using the identities that $\text{Var}[\ell^{y_r}|\mathbf{x}] = \mathbb{E}[(\ell^{y_r})^2|\mathbf{x}] - \mathbb{E}^2[\ell^{y_r}|\mathbf{x}]$ and $\text{Cov}[\ell^{y_r}, \ell^{y_s}|\mathbf{x}] = \mathbb{E}[\ell^{y_r} \cdot \ell^{y_s}|\mathbf{x}] - \mathbb{E}[\ell^{y_r}|\mathbf{x}] \cdot \mathbb{E}[\ell^{y_s}|\mathbf{x}]$. \square

B Label Distribution Prediction Results

Tables 5-9 show the label distribution prediction performance measured by Chebyshev distance, Clark distance, Canberra metric, Kullback-Leibler divergence and Intersection, respectively, as the averaged scores on ten-fold cross-validation. On each dataset, the best performer and runner-up are respectively highlighted by **boldface** and underline. We perform paired t tests between the proposed SNEFY-LDL and every baseline method, and use symbols \bullet , \circ and \spadesuit to respectively denote that SNEFY-LDL is superior, inferior and equivalent to the baseline at 0.05 significance level. The last column Δ gives the performance difference between SNEFY-LDL and the best baseline. The scores in Tables 5-9 consistently confirm that SNEFY-LDL is very competitive compared with the state-of-the-art baselines.

Dataset	PT-SVM	AA-KNN	CPNN	SA-BFGS	LDLF	DF-LDL	LDL-SCL	LDL-LRR	SNEFY-LDL	Δ
Movie	0.1183 \bullet	0.1193 \bullet	0.1330 \bullet	0.1163 \spadesuit	0.1668 \bullet	0.1135 \circ	0.1444 \bullet	<u>0.1154</u> \circ	0.1172	+0.0037
Natural_Scene	0.3104 \spadesuit	0.3130 \spadesuit	0.3563 \bullet	0.3194 \spadesuit	0.3023 \spadesuit	0.3077 \spadesuit	0.3603 \bullet	<u>0.3046</u> \spadesuit	0.3135	+0.0112
SBU_3DFE	0.1300 \bullet	0.1277 \bullet	0.1394 \bullet	0.1152 \bullet	0.1197 \bullet	<u>0.1147</u> \bullet	0.1303 \bullet	0.1268 \bullet	0.1110	-0.0037
SJAFFE	0.1158 \bullet	0.0975 \spadesuit	0.1202 \bullet	0.0921 \spadesuit	0.0862 \circ	0.0810 \circ	0.0868 \circ	<u>0.0831</u> \circ	0.0997	+0.0188
Yeast_alpha	0.0140 \bullet	0.0144 \bullet	0.0140 \bullet	<u>0.0134</u> \circ	0.0138 \spadesuit	0.0134 \circ	0.0135 \circ	0.0134 \circ	0.0137	+0.0003
Yeast_cdc	0.0168 \spadesuit	0.0172 \bullet	0.0169 \bullet	0.0162 \circ	0.0163 \circ	0.0162 \circ	0.0164 \circ	<u>0.0162</u> \circ	0.0167	+0.0005
Yeast_cold	0.0529 \bullet	0.0542 \bullet	0.0538 \bullet	<u>0.0512</u> \spadesuit	0.0535 \bullet	0.0514 \spadesuit	0.0543 \bullet	0.0512 \spadesuit	0.0518	+0.0006
Yeast_diau	0.0386 \spadesuit	0.0384 \spadesuit	0.0407 \bullet	<u>0.0369</u> \circ	0.0376 \spadesuit	0.0369 \circ	0.0405 \bullet	0.0370 \circ	0.0382	+0.0013
Yeast_dtt	0.0381 \bullet	0.0385 \bullet	0.0370 \spadesuit	0.0360 \circ	0.0374 \spadesuit	0.0365 \spadesuit	0.0393 \spadesuit	<u>0.0360</u> \circ	0.0369	+0.0009
Yeast_elu	0.0171 \bullet	0.0173 \bullet	0.0169 \spadesuit	<u>0.0163</u> \circ	0.0163 \circ	0.0162 \circ	0.0164 \circ	0.0163 \circ	0.0168	+0.0005
Yeast_heat	0.0438 \bullet	0.0440 \bullet	0.0433 \bullet	0.0422 \spadesuit	0.0425 \spadesuit	0.0420 \circ	0.0435 \spadesuit	<u>0.0422</u> \spadesuit	0.0425	+0.0006
Yeast_spo	0.0589 \bullet	0.0629 \bullet	0.0593 \bullet	0.0584 \spadesuit	0.0612 \bullet	0.0603 \bullet	0.0592 \bullet	<u>0.0583</u> \spadesuit	0.0583	-0.0000
Yeast_spo5	0.0923 \bullet	0.0952 \bullet	0.0920 \bullet	0.0913 \spadesuit	0.0998 \bullet	0.0973 \bullet	0.1083 \bullet	<u>0.0912</u> \spadesuit	0.0910	-0.0002
Yeast_spoem	0.0884 \bullet	0.0907 \bullet	0.0874 \spadesuit	0.0868 \spadesuit	0.0932 \bullet	0.1043 \bullet	0.2315 \bullet	<u>0.0865</u> \spadesuit	0.0865	-0.0000

Table 5: The comparison of label distribution prediction performance measured by Chebyshev distance.

Dataset	PT-SVM	AA-KNN	CPNN	SA-BFGS	LDLF	DF-LDL	LDL-SCL	LDL-LRR	SNEFY-LDL	Δ
Movie	0.5293 ◦	0.5312 ♠	0.5636 ●	0.5251 ◦	0.7024 ●	0.5107 ◦	0.6230 ●	<u>0.5214</u> ◦	0.5370	+0.0263
Natural_Scene	2.4441 ◦	1.9084 ◦	2.4878 ●	2.4234 ◦	2.4313 ◦	2.4130 ◦	<u>2.3683</u> ◦	2.4399 ◦	2.4568	+0.5484
SBU_3DFE	0.4067 ●	0.4015 ●	0.4151 ●	0.3710 ●	0.3770 ●	<u>0.3624</u> ●	0.4025 ●	0.3975 ●	0.3429	-0.0195
SJAFFE	0.4167 ●	0.3477 ♠	0.4293 ●	0.3589 ♠	0.3350 ◦	0.3031 ◦	0.3222 ◦	<u>0.3149</u> ◦	0.3613	+0.0582
Yeast_alpha	0.2218 ●	0.2261 ●	0.2239 ●	<u>0.2099</u> ◦	0.2166 ♠	0.2094 ◦	0.2122 ◦	<u>0.2099</u> ◦	0.2182	+0.0088
Yeast_cdc	0.2255 ●	0.2317 ●	0.2243 ●	<u>0.2158</u> ◦	0.2173 ◦	0.2157 ◦	0.2179 ◦	0.2159 ◦	0.2219	+0.0062
Yeast_cold	0.1443 ●	0.1477 ●	0.1458 ●	<u>0.1396</u> ♠	0.1456 ●	0.1405 ♠	0.1479 ●	0.1396 ♠	0.1411	+0.0015
Yeast_diau	0.2096 ●	0.2080 ♠	0.2178 ●	<u>0.2007</u> ◦	0.2032 ♠	0.2001 ◦	0.2213 ◦	0.2007 ◦	0.2070	+0.0068
Yeast_dtt	0.1041 ●	0.1042 ●	0.1008 ♠	0.0982 ◦	0.1017 ♠	0.0994 ♠	0.1065 ♠	<u>0.0982</u> ◦	0.1006	+0.0025
Yeast_elu	0.2114 ●	0.2131 ●	0.2073 ♠	<u>0.1990</u> ◦	0.2003 ◦	0.1985 ◦	0.2014 ◦	0.1990 ◦	0.2077	+0.0092
Yeast_heat	0.1893 ●	0.1908 ●	0.1876 ●	<u>0.1826</u> ♠	0.1844 ♠	0.1815 ◦	0.1882 ●	0.1826 ♠	0.1839	+0.0024
Yeast_spo	0.2530 ●	0.2665 ●	0.2533 ●	0.2498 ♠	0.2594 ●	0.2552 ●	0.2530 ●	<u>0.2497</u> ♠	0.2494	-0.0003
Yeast_spo5	0.1861 ●	0.1915 ●	0.1857 ●	0.1840 ♠	0.1999 ●	0.1951 ●	0.2145 ●	<u>0.1838</u> ♠	0.1833	-0.0005
Yeast_spoem	0.1313 ●	0.1350 ●	0.1299 ♠	0.1292 ♠	0.1392 ●	0.1541 ●	0.3628 ●	0.1287 ♠	<u>0.1288</u>	+0.0001

Table 6: The comparison of label distribution prediction performance measured by Clark distance \downarrow .

Dataset	PT-SVM	AA-KNN	CPNN	SA-BFGS	LDLF	DF-LDL	LDL-SCL	LDL-LRR	SNEFY-LDL	Δ
Movie	1.0116 ♠	1.0205 ♠	1.0588 ●	1.0055 ♠	1.4036 ●	0.9796 ◦	1.1795 ●	<u>0.9970</u> ◦	1.0154	+0.0357
Natural_Scene	6.7001 ♠	4.5465 ◦	6.9670 ●	6.6520 ◦	6.6519 ♠	6.5907 ◦	<u>6.5539</u> ◦	6.6785 ◦	6.7202	+2.1737
SBU_3DFE	0.8713 ●	0.8306 ●	0.9055 ●	0.7827 ●	0.8035 ●	<u>0.7638</u> ●	0.8580 ●	0.8485 ●	0.7347	-0.0291
SJAFFE	0.8604 ●	0.7148 ♠	0.9001 ●	0.7326 ♠	0.6820 ◦	0.6188 ◦	0.6648 ◦	<u>0.6421</u> ◦	0.7473	+0.1285
Yeast_alpha	0.7237 ●	0.7388 ●	0.7327 ●	<u>0.6818</u> ◦	0.7051 ♠	0.6802 ◦	0.6911 ◦	0.6819 ◦	0.7128	+0.0325
Yeast_cdc	0.6794 ●	0.7001 ●	0.6733 ♠	<u>0.6473</u> ◦	0.6524 ◦	0.6472 ◦	0.6540 ◦	0.6475 ◦	0.6673	+0.0202
Yeast_cold	0.2487 ●	0.2550 ●	0.2515 ●	<u>0.2403</u> ♠	0.2513 ●	0.2424 ♠	0.2558 ●	0.2403 ♠	0.2430	+0.0027
Yeast_diau	0.4501 ●	0.4476 ♠	0.4671 ●	0.4308 ◦	0.4367 ♠	0.4300 ◦	0.4804 ●	<u>0.4308</u> ◦	0.4449	+0.0149
Yeast_dtt	0.1796 ●	0.1789 ●	0.1732 ♠	0.1689 ◦	0.1750 ♠	0.1711 ♠	0.1832 ♠	<u>0.1689</u> ◦	0.1731	+0.0043
Yeast_elu	0.6236 ●	0.6281 ●	0.6084 ♠	<u>0.5831</u> ◦	0.5876 ◦	0.5820 ◦	0.5905 ◦	0.5832 ◦	0.6116	+0.0296
Yeast_heat	0.3780 ●	0.3834 ●	0.3739 ●	<u>0.3641</u> ◦	0.3688 ♠	0.3626 ◦	0.3763 ●	0.3642 ◦	0.3670	+0.0044
Yeast_spo	0.5199 ●	0.5489 ●	0.5223 ●	<u>0.5131</u> ♠	0.5346 ●	0.5245 ●	0.5218 ●	0.5129 ♠	0.5143	+0.0014
Yeast_spo5	0.2856 ●	0.2945 ●	0.2847 ●	0.2826 ♠	0.3082 ●	0.3003 ●	0.3344 ●	<u>0.2824</u> ♠	0.2820	-0.0004
Yeast_spoem	0.1828 ●	0.1878 ●	0.1807 ♠	0.1797 ♠	0.1934 ●	0.2149 ●	0.4967 ●	0.1791 ♠	<u>0.1792</u>	+0.0001

Table 7: The comparison of label distribution prediction performance measured by Canberra metric \downarrow .

Dataset	PT-SVM	AA-KNN	CPNN	SA-BFGS	LDLF	DF-LDL	LDL-SCL	LDL-LRR	SNEFY-LDL	Δ
Movie	0.1011 ●	0.1093 ●	0.1113 ●	0.1002 ●	0.2357 ●	0.0975 ▲	0.1380 ●	<u>0.0981</u> ▲	0.0984	+0.0009
Natural_Scene	<u>0.7608</u> ▲	1.0936 ●	1.0466 ●	0.8277 ▲	0.7832 ▲	0.7608 ▲	1.0478 ●	0.7445 ▲	0.7704	+0.0259
SBU_3DFE	0.0774 ●	0.0803 ●	0.0860 ●	0.0629 ●	0.0651 ●	<u>0.0620</u> ●	0.0776 ●	0.0730 ●	0.0578	-0.0042
SJAFFE	0.0701 ●	0.0534 ▲	0.0740 ●	0.0505 ▲	0.0446 ○	0.0375 ○	0.0419 ○	<u>0.0391</u> ○	0.0523	+0.0148
Yeast_alpha	0.0060 ●	0.0063 ●	0.0061 ●	<u>0.0055</u> ○	0.0058 ▲	0.0055 ○	0.0056 ○	0.0055 ○	0.0059	+0.0004
Yeast_cdc	0.0075 ●	0.0079 ●	0.0076 ●	<u>0.0070</u> ○	0.0071 ○	0.0070 ○	0.0071 ○	0.0070 ○	0.0073	+0.0004
Yeast_cold	0.0128 ●	0.0136 ●	0.0132 ●	<u>0.0122</u> ○	0.0132 ●	0.0123 ▲	0.0137 ●	0.0122 ○	0.0124	+0.0002
Yeast_diau	0.0142 ●	0.0145 ▲	0.0151 ●	<u>0.0131</u> ○	0.0138 ▲	0.0132 ○	0.0165 ●	0.0131 ○	0.0138	+0.0007
Yeast_dtt	0.0069 ●	0.0070 ●	0.0065 ▲	0.0063 ○	0.0068 ▲	0.0064 ▲	0.0072 ▲	<u>0.0063</u> ○	0.0065	+0.0002
Yeast_elu	0.0069 ●	0.0071 ●	0.0066 ▲	<u>0.0062</u> ○	0.0063 ○	0.0062 ○	0.0063 ○	0.0062 ○	0.0066	+0.0005
Yeast_heat	0.0135 ●	0.0139 ●	0.0133 ●	0.0126 ○	0.0130 ▲	0.0125 ○	0.0133 ▲	<u>0.0126</u> ○	0.0129	+0.0004
Yeast_spo	0.0251 ▲	0.0289 ●	0.0258 ●	<u>0.0246</u> ○	0.0271 ●	0.0259 ●	0.0257 ●	0.0246 ○	0.0251	+0.0005
Yeast_spo5	0.0298 ●	0.0326 ●	0.0297 ●	0.0292 ▲	0.0351 ●	0.0338 ●	0.0409 ●	<u>0.0292</u> ▲	0.0290	-0.0002
Yeast_spoem	0.0253 ●	0.0274 ●	0.0247 ▲	<u>0.0245</u> ▲	0.0301 ●	0.0346 ●	0.1475 ●	0.0245 ▲	0.0243	-0.0002

Table 8: The comparison of label distribution prediction performance measured by Kullback-Leibler divergence \downarrow .

Dataset	PT-SVM	AA-KNN	CPNN	SA-BFGS	LDLF	DF-LDL	LDL-SCL	LDL-LRR	SNEFY-LDL	Δ
Movie	0.8324 ▲	0.8294 ●	0.8196 ●	0.8336 ▲	0.7572 ●	0.8380 ○	0.7953 ●	<u>0.8353</u> ○	0.8333	-0.0048
Natural_Scene	0.5549 ▲	0.5629 ○	0.4153 ●	0.5491 ▲	0.5536 ▲	0.5566 ▲	0.5294 ▲	<u>0.5595</u> ○	0.5343	-0.0286
SBU_3DFE	0.8436 ●	0.8484 ●	0.8380 ●	0.8600 ●	0.8559 ●	<u>0.8624</u> ●	0.8456 ●	0.8477 ●	0.8685	+0.0061
SJAFFE	0.8523 ●	0.8768 ▲	0.8466 ●	0.8786 ▲	0.8865 ○	0.8959 ○	0.8876 ○	<u>0.8928</u> ○	0.8729	-0.0229
Yeast_alpha	0.9600 ●	0.9592 ●	0.9595 ●	<u>0.9624</u> ○	0.9611 ▲	0.9624 ○	0.9618 ○	0.9624 ○	0.9606	-0.0018
Yeast_cdc	0.9552 ●	0.9539 ●	0.9557 ▲	<u>0.9574</u> ○	0.9571 ○	0.9574 ○	0.9570 ○	0.9574 ○	0.9561	-0.0014
Yeast_cold	0.9387 ●	0.9371 ●	0.9379 ●	<u>0.9408</u> ▲	0.9380 ●	0.9403 ▲	0.9368 ●	0.9408 ▲	0.9401	-0.0007
Yeast_diau	0.9375 ●	0.9379 ▲	0.9350 ●	0.9403 ○	0.9394 ▲	0.9404 ○	0.9334 ●	<u>0.9403</u> ○	0.9383	-0.0021
Yeast_dtt	0.9556 ●	0.9559 ●	0.9572 ▲	0.9583 ○	0.9568 ▲	0.9578 ▲	0.9547 ▲	<u>0.9583</u> ○	0.9573	-0.0011
Yeast_elu	0.9560 ●	0.9557 ●	0.9571 ▲	<u>0.9589</u> ○	0.9585 ○	0.9589 ○	0.9583 ○	0.9589 ○	0.9568	-0.0021
Yeast_heat	0.9379 ●	0.9371 ●	0.9386 ●	<u>0.9402</u> ○	0.9395 ▲	0.9405 ○	0.9382 ●	0.9402 ○	0.9397	-0.0008
Yeast_spo	0.9144 ●	0.9094 ●	0.9140 ●	<u>0.9155</u> ▲	0.9118 ●	0.9135 ●	0.9140 ●	0.9156 ▲	0.9153	-0.0002
Yeast_spo5	0.9077 ●	0.9048 ●	0.9080 ●	0.9087 ▲	0.9002 ●	0.9027 ●	0.8917 ●	<u>0.9088</u> ▲	0.9090	+0.0002
Yeast_spoem	0.9116 ●	0.9093 ●	0.9126 ▲	0.9132 ▲	0.9068 ●	0.8957 ●	0.7685 ●	<u>0.9135</u> ▲	0.9135	+0.0000

Table 9: The comparison of label distribution prediction performance measured by Intersection \uparrow .

C Parameter Sensitivity Study

On the *Movie* and *SBU_3DFE* datasets, we take turns to study the sensitivity of SNEFY-LDL with regard to the four hyperparameters: n and m , as well as the batch size and epoch number used for training, by varying the studied hyperparameter in a predefined range and fixing the remaining three as default values at each turn. Figure 1 plots the performance change of SNEFY-LDL measured by Cosine coefficient with the varying values of the four hyperparameters. From Figure 1, we can find that the performance of SNEFY-LDL remains relatively stable when the hyperparameters vary in proper ranges.

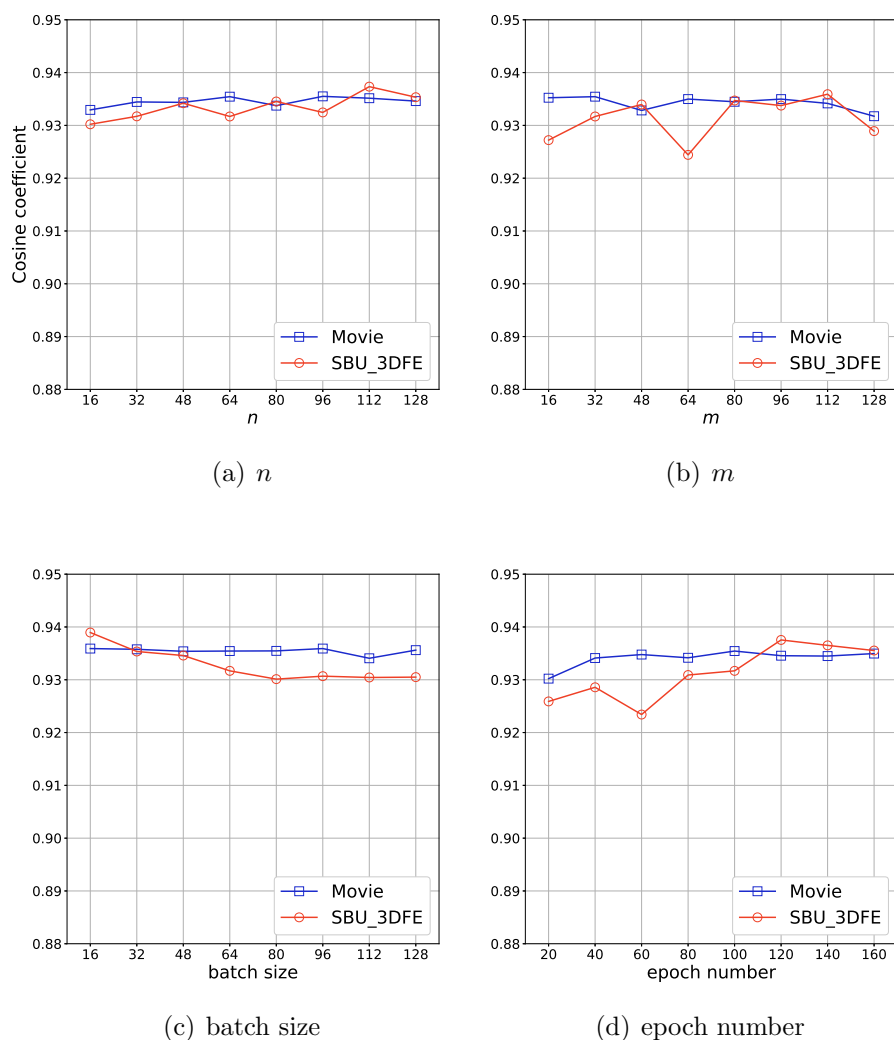


Figure 1: Parameter sensitivity.